



# Geochemical Characteristics and Origin of Shale Gases From Sichuan Basin, China

Yunyan Ni<sup>1\*</sup>, Dazhong Dong<sup>1\*</sup>, Limiao Yao<sup>1</sup>, Jianping Chen<sup>1</sup>, Xing Liang<sup>2</sup>, Fei Liu<sup>2</sup>, Jian Li<sup>1</sup>, Jinhao Guo<sup>1</sup> and Jinliang Gao<sup>1</sup>

<sup>1</sup>PetroChina Research Institute of Petroleum Exploration and Development, Beijing, China, <sup>2</sup>PetroChina Zhejiang Oilfield Company, Hangzhou, China

## OPEN ACCESS

### Edited by:

Qingqiang Meng,  
SINOPEC Petroleum Exploration and  
Production Research Institute, China

### Reviewed by:

Xiaofeng Wang,  
Northwest University, China  
Haikuan Nie,  
SINOPEC Petroleum Exploration and  
Production Research Institute, China

### \*Correspondence:

Yunyan Ni  
niyy@petrochina.com.cn  
Dazhong Dong  
ddz@petrochina.com.cn

### Specialty section:

This article was submitted to  
Geochemistry,  
a section of the journal  
Frontiers in Earth Science

Received: 24 January 2022

Accepted: 09 May 2022

Published: 22 June 2022

### Citation:

Ni Y, Dong D, Yao L, Chen J, Liang X,  
Liu F, Li J, Guo J and Gao J (2022)  
Geochemical Characteristics and  
Origin of Shale Gases From Sichuan  
Basin, China.  
Front. Earth Sci. 10:861040.  
doi: 10.3389/feart.2022.861040

Natural gases from the Taiyang (shallow), Jiaoshiba (middle), and Weirong (deep) shale gas fields in the southern Sichuan Basin were analyzed for molecular and stable carbon isotopic compositions to investigate the geochemical characteristics and gas origins. All the gases belong to shale gas from the Upper Ordovician–Lower Silurian shale and are dominated by methane with gas wetness generally less than 0.83%. The  $\delta^{13}\text{C}_1$  values are  $-28.5\text{‰}$ ,  $-30.3\text{‰}$ , and  $-35.2\text{‰}$  in Taiyang, Jiaoshiba, and Weirong shale gas fields, respectively. The extremely high thermal maturity is the controlling factor for the enrichment of  $^{13}\text{C}$  in methane, with a minor contribution from the heavy carbon isotope of the organic matter in the Ordovician Wufeng Formation. Fischer–Tropsch-type synthesis of hydrocarbon gas from  $\text{CO}_2$  and  $\text{H}_2$  contributes to the increase of wet gas, which results in the offset from the  $\delta^{13}\text{C}_1$ –wetness linear trend in the Taiyang and Jiaoshiba gas fields. Methane, ethane, and propane in the Taiyang shale gas field have increasing  $\delta^{13}\text{C}$  values with increasing burial depth, which is mainly caused by diffusive migration. All gases are characterized by a complete carbon isotopic reversal trend ( $\delta^{13}\text{C}_1 > \delta^{13}\text{C}_2 > \delta^{13}\text{C}_3$ ), and it is mainly caused by the reversible free-radical reactions with the conversion from alkane to alkyl groups, with some contribution from the Fischer–Tropsch-type synthesis. The results of this study will improve our understanding of the geochemical characteristics of shale gases from different burial depths and have important implications for future shale gas exploration in the deep and shallow layers.

**Keywords:** shale gas, carbon isotope reversal, Wufeng–Longmaxi shale, Sichuan Basin, carbon isotope enrichment

## 1 INTRODUCTION

Carbon isotopic compositions of methane and its homologs are important parameters to investigate the origin and generation history of natural gas (Tang et al., 2000; Ni et al., 2011; Dai et al., 2014a). Several studies have shown that the carbon isotope is dependent on the maturity of source rocks, the type and carbon isotope of source organic matter, and postgenetic processes (Stahl and Carey, 1975; Schoell, 1980; Dai, 1992; Tang et al., 2000; Dai et al., 2009; Ni et al., 2011; Curiale and Curtis, 2016; Ni et al., 2019a). Due to the kinetic isotopic fractionation effects (Lorant et al., 1998; Tang et al., 2000), primary gases are usually characterized by the normal carbon isotopic trend, that is,  $\delta^{13}\text{C}_1 < \delta^{13}\text{C}_2 < \delta^{13}\text{C}_3$ . However, recently, a number of studies have documented a depletion of  $^{13}\text{C}$  in ethane and propane and an enrichment of  $^{13}\text{C}$  in methane at high maturity, resulting in the carbon isotopic reversal between methane and ethane ( $\delta^{13}\text{C}_1 > \delta^{13}\text{C}_2$ ) (Ferworn et al., 2008; Burruss and Laughrey,

2010; Rodriguez and Philp, 2010; Zumberge et al., 2012; Hao and Zou, 2013; Tilley and Muehlenbachs, 2013; Dai et al., 2014a, 2016b, 2017; Zhang et al., 2018b; Liu et al., 2018; Ni et al., 2018; Xia and Gao, 2018; Feng et al., 2020).

Zumberge et al. (2012) demonstrated a reversed carbon isotopic maturity trend in ethane and propane in gases from Barnett and Fayetteville shales, with thermal maturity (Ro%) over 1.5%. Dai et al. (2014b) explored this reversed trend to even higher thermal maturity and found the carbon isotopic maturity trend becomes positive again at stages with gas wetness ( $C_{2+}/C_{1+}$ , %) less than 1.4%. Ni et al. (2018) show such isotopic depletion of  $^{13}C$  in thermogenic ethane and propane. One common feature of these carbon isotopic anomalies is that they occur at relatively high temperatures. To date, many studies have been carried out to investigate the mechanisms for the carbon isotopic characteristics of shale gases (Ferworn et al., 2008; Burruss and Laughrey, 2010; Rodriguez and Philp, 2010; Zumberge et al., 2012; Hao and Zou, 2013; Xia et al., 2013; Gao et al., 2014; Zhang et al., 2018b; Xia and Gao, 2018; Feng et al., 2020; Mi et al., 2022). Moreover, isotopic reversal may correlate with the gas generation potential, and the reversal magnitude may correspond to the amount of gas retained in the shale (Tilley et al., 2011; Feng et al., 2018; Wang et al., 2021; Zhao et al., 2021).

As the largest shale gas producer outside North America, after 10-years effort, China has achieved effective exploitation of marine shale gas resources in the Sichuan Basin and its surrounding areas with a middle burial depth of 2,000–3,500 m. In the Sichuan Basin, ultra-deep shale gas represents shale gas with a burial depth >4,500 m, deep shale gas means shale gas with a burial depth of 3,500–4,500 m, and shallow shale gas means shale gas with a burial depth <2,000 m. With the success of the burial depth of 2,000–3,500 m, recently, great efforts have been made in the shallow and deep layers. In the future, with the improvement of the technologies, shale gas exploration will extend to areas shallower than 2,000 m and deeper than 3,500 m. How about the geochemistry of shale gas from shallow and deep layers? Are there any differences among the shale gases from the shallow, middle, and deep layers? Here, we describe the molecular and stable carbon isotope geochemistry of natural gases from the Wufeng–Longmaxi shale in the Taiyang (vertical burial depth, 500–2,250 m), Jiaoshiba (vertical burial depth, 2,250–3,500 m) and Weirong (vertical burial depth, 3,550–3,880 m) shale gas fields in the Sichuan Basin. Two main objectives of this study will be addressed: 1) Investigating the origin of the shale gases from the three gas fields with different burial depths based on the molecular and stable carbon isotopic compositions and 2) demonstrating the geochemical differences among shale gases from these three gas fields and exploring the potential causes. The results presented in this study will improve our understanding of the geochemical differences among the shale gases with deep, middle, and shallow burial depths and interpretation of the carbon isotopic composition of shale gases in the future.

## 2 GEOLOGICAL SETTINGS

The Sichuan Basin, abundant in natural gas resources, is a large superimposed basin and covers an area of about  $180 \times 10^3 \text{ km}^2$

(Figure 1). The sedimentary strata are well-developed with thicknesses up to 12,000 m. It developed nine sets of gas source rocks and has found 25 conventional and tight gas-producing zones (18 being marine facies) and one marine facies shale gas-producing zone. The nine sets of gas source rocks include the Sinian Doushantuo and Dengying formations, Cambrian Qiongzhusi Formation, Upper Ordovician Wufeng–Lower Silurian Longmaxi formations, Permian Qixia, Maokou, Dalong, Longtan/Wujiaping formations, and Triassic Xujiahe Formation (Figure 2). The former seven sets belong to marine sapropelic source rocks. The Sinian Doushantuo and Dengying formations were deposited during a sea transgression. It is distributed mainly in the basin margins in the northwest, northeast, and southeast of the Sichuan Basin, with very thin thickness in the basin. The Cambrian Qiongzhusi Formation is characterized by black carbonaceous shale with an average thickness of 180 m in the basin. The organic matter is dominated by Type I and Type II<sub>1</sub> kerogen with total organic content (TOC) up to 6% in the southern and northern Sichuan, and the thermal maturity equivalent Ro% is 2%–5% (Xu et al., 2011). The Permian Qixia and Maokou formations are a set of carbonate deposits and are widely distributed in the basin with thickness between 150–400 m and TOC generally less than 2% (Huang et al., 2016). The Permian Dalong Formation is a set of black mudstone and siliceous mudstone. It is mainly distributed in the northern Sichuan Basin with a thickness up to 30 m (Xia et al., 2013). It has a TOC between 0.43%–21.2% (average = 8.3%,  $n = 38$ ) and  $\delta^{13}C$  values of kerogen from  $-24\text{‰}$  to  $-29\text{‰}$  (Chen et al., 2018). The Longtan Formation/Wujiaping Formation belongs to marine-continental transitional source rocks, where the Longtan Formation is a set of coal measure gas source rocks, similar to the Xujiahe Formation. Wujiaping Formation is contemporaneous with Longtan Formation, but mainly a set of marine sapropelic source rocks. The Triassic Xujiahe Formation is dominated by Type II<sub>2</sub> and Type III organic matter, which is a set of coal measure gas source rocks. The Wufeng–Longmaxi formations are the only industrial exploration and development strata of shale gas. The Wufeng Formation has a thickness of 2–11 m, and the Longmaxi hot shale is concentrated on the bottom 10–40 m of the Lower Longmaxi Formation. The Wufeng–Longmaxi hot shale has a burial depth of 500–5,500 m and is deposited in an environment of deep water shelf facies and stably distributed. By 2020, Jiaoshiba, Changning, Weiyuan, Huangjinba, Taiyang, Weirong, Yongchuan, and other shale gas fields have been discovered (Figure 1). In China, the cumulative proved geological reserves of shale gas were  $2.0 \times 10^{12} \text{ m}^3$ , the completed production capacity was  $300 \times 10^8 \text{ m}^3/\text{year}$ , and the annual shale gas output was  $200.55 \times 10^8 \text{ m}^3$  in 2020.

### 2.1 Taiyang Shale Gas Field

The Taiyang shale gas field is located in the south of Xuyong County, Sichuan Province, and is a part of the Zhaotong National Shale Gas Demonstration Zone (Figure 1). It belongs to the Taiyang anticline, which was a narrow and steep anticlinal structure cut and damaged by strike-slip faults. It has been uplifted continuously since the Late Jurassic, and

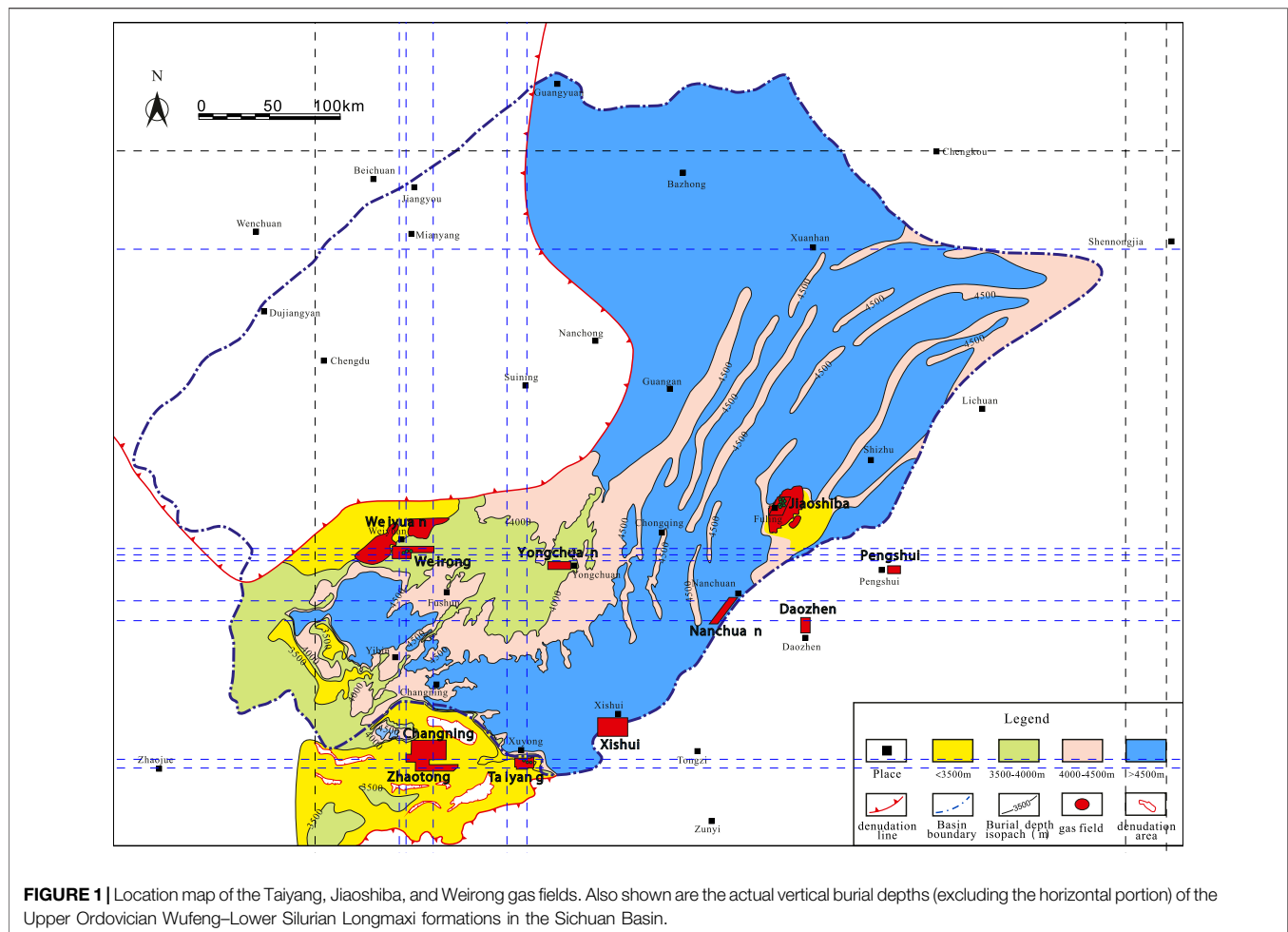
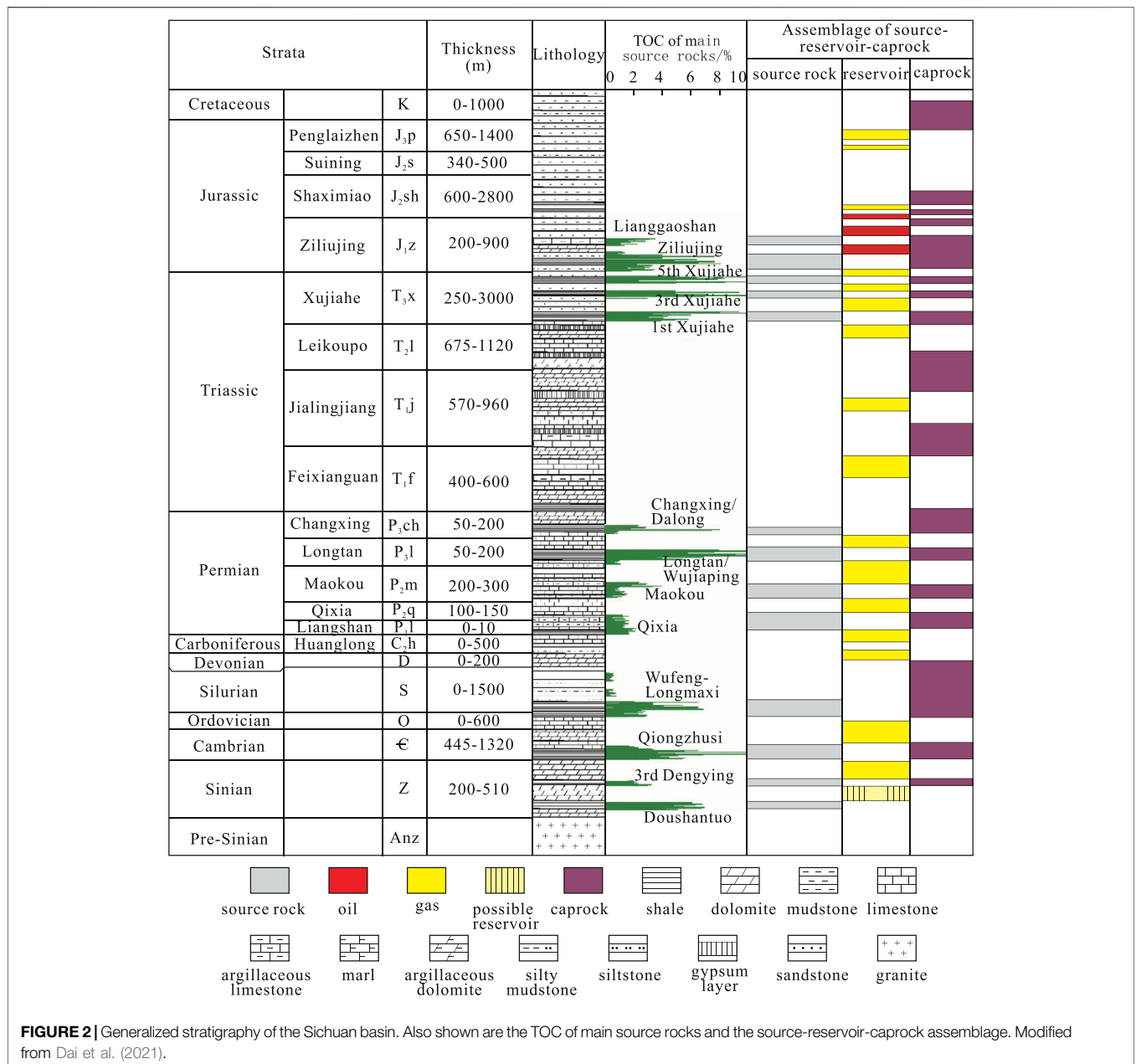


**FIGURE 1** | Location map of the Taiyang, Jiaoshiba, and Weirong gas fields. Also shown are the actual vertical burial depths (excluding the horizontal portion) of the Upper Ordovician Wufeng–Lower Silurian Longmaxi formations in the Sichuan Basin.

the uplifted range is about 2,000 m, which resulted in the denudation of the strata above Permian and possible loss of free gas. The black organic-rich siliceous shale and carbonaceous shale of the Wufeng–Longmaxi formations are the main targets of the shale gas field development, with a vertical burial depth (excluding the horizontal portion) of 500–2,250 m and formation pressure coefficient of 1.2–1.47, which belongs to shallow, atmospheric-overpressure shale gas reservoirs. The high-quality reservoirs are 13–18 m thick and stable in distribution, with TOC content of 0.42%–9.05% with an average of 2.92%. The organic matter is dominated by Type II<sub>1</sub>, and the equivalent Ro% ranges from 3.0% to 3.9% (average = 3.45%) (Wang et al., 2019; Liang et al., 2021; Zou et al., 2021). The shale porosity is 2.92%–8.01%, with an average of 4.98%. The average brittleness is 72%, the gas content is 3.3–5.51 m<sup>3</sup>/t, and the average content of clay minerals is 24.7%. By the end of 2020, the accumulative proved reserves had been  $1,365 \times 10^8$  m<sup>3</sup>. The completed production capacity was  $8 \times 10^8$  m<sup>3</sup>/year, and the annual shale gas output was  $4.0 \times 10^8$  m<sup>3</sup> in 2020.

## 2.2 Jiaoshiba Shale Gas Field

The Jiaoshiba shale gas field is located in the east of Chongqing and is a part of the Fuling National Shale Gas Demonstration Zone (Figure 1). It has an area of about 575.92 km<sup>2</sup>. The main body of the Jiaoshiba gas field is a box anticlinal structure spreading NE–SW, with faults controlling the east and west sides and large-scale faults developing in the southeast. The uplift was late and large, about 3,000 m, and the limestone of the Triassic Jialingjiang Formation is exposed, but the gas reservoir is well-preserved. The Wufeng–Longmaxi organic-rich shale is the main target layer of the shale gas field. The optimal reservoir section has a burial depth (excluding the horizontal portion) of 2,250–3,500 m. It is stably distributed with a thickness of about 38–40 m and a pressure coefficient of 1.55. It is dominated by Type I organic matter with an average TOC of 3.76%, porosity of 4.87%, brittleness of 62.4%, gas content of 2.96 m<sup>3</sup>/t, clay mineral content of 31.6%, and equivalent Ro% of 3.1% (2.6%–3.6%) (Dai et al., 2014a; Wang et al., 2019; Zou et al., 2021). By the end of 2020, the accumulative proved reserves had been  $6008.14 \times 10^8$  m<sup>3</sup>. The completed production capacity



was  $100 \times 10^8 \text{ m}^3/\text{year}$ , and the annual shale gas production was  $67 \times 10^8 \text{ m}^3$  in 2020.

### 2.3 Weirong Shale Gas Field

The Weirong shale gas field is located in Neijiang and Zigong counties of Sichuan Province and is a part of the Changning–Weiyuan National Shale Gas Demonstration Zone (Figure 1). The main body of the gas field belongs to the Baimazhen syncline of the low-fold structural belt in southwestern Sichuan. The structure is gentle, and the fault is not developed. Influenced by the uplift evolution of the

Sichuan Basin in the Late Cretaceous, the Jurassic was exposed on the surface, and the burial depth (excluding the horizontal portion) of the gas layer was 3,550–3,880 m. The overall preservation condition of the gas layer is good, and the formation pressure is high, that is, 1.94–2.06. The high-quality reservoirs are 25–39 m thick and stable in distribution, with an average TOC of 2.80%, porosity of 6.07%, brittleness of 64%, gas content of  $3.15 \text{ m}^3/\text{t}$ , clay mineral content of 34%, and equivalent  $R_o\%$  of 2.25% (1.8%–2.7%) (Wang et al., 2019; Zou et al., 2021). By the end of 2020, the cumulative proved reserves had been 1,247

$\times 10^8 \text{ m}^3$ . The completed production capacity was  $10 \times 10^8 \text{ m}^3$ /year, and the annual shale gas output was  $5.4 \times 10^8 \text{ m}^3$  in 2020.

### 3 SAMPLES AND METHODS

Eleven shale gas samples from the Weirong shale gas field in the Changning–Weiyuan National Shale Gas Demonstration Zone (marked as Weirong), 10 shale gas samples from the Taiyang shale gas field in the Zhaotong National Shale Gas Demonstration Zone (marked as Taiyang), and 10 shale gas samples from the Jiaoshiba shale gas field in the Fuling National Shale Gas Demonstration Zone (marked as Jiaoshiba) were collected (Figure 1).

Samples were pure gases and collected directly from the wellheads or separators in the shale fields. Double-ended stainless steel bottles (10 cm diameter about  $1,000 \text{ cm}^3$  volume) were used to collect the samples, which were equipped with shut-off valves with a maximum pressure of 22.5 MPa. The bottles and the lines were flushed with the sample gases for 15–20 min to remove air contamination. The pressure inside the bottle was kept above atmospheric pressure. Leakage tests by immersing bottles in a water bath were performed for all samples.

The molecular and isotopic compositions of the gas samples were determined at the PetroChina Research Institute of Petroleum Exploration and Development (RIPED). The molecular composition was determined using an Agilent 7890A gas chromatograph, which was equipped with a flame ionization detector and a thermal conductivity detector. Gas components were separated using six columns (2 Foot 12% UCW982 on PAW 80/100 mesh, 15 Foot 25% DC200 on PAW 80/100 mesh, 10 Foot Hayesep 80/100 mesh, 10 Foot Molecular Sieve 13X 45/60 mesh, 8 Foot Molecular Sieve 5A 60/80 mesh, and 3 Foot Hayesep Q 80/100 mesh). GC oven temperature was set at  $85^\circ\text{C}$  for 40 min. Immediately prior to the molecular composition analysis, the GC is calibrated by certified gas standards, which is also used to monitor the analytical drift by injecting them before, during, and after the analysis. The analytical precision and accuracy are typically better than 0.01% for methane, ethane, and propane.

Stable carbon isotopes were determined using a Thermo Delta V mass spectrometer, which was interfaced with a Thermo Trace GC Ultra gas chromatograph (GC). Methane, ethane, propane, and  $\text{CO}_2$  were separated on a gas chromatograph using a fused silica capillary column (PLOT Q  $27.5 \text{ m} \times 0.32 \text{ mm} \times 10 \mu\text{m}$ ), converted into  $\text{CO}_2$  in a combustion interface, and then injected into the mass spectrometer. The temperature programming of the GC oven was as follows: heated from  $33^\circ\text{C}$  to  $80^\circ\text{C}$  at  $8^\circ\text{C}/\text{min}$ , then to  $250^\circ\text{C}$  at  $5^\circ\text{C}/\text{min}$ , and maintained at  $250^\circ\text{C}$  for 10 min. An oil-related gas from the Tazhong gas field in the Tarim Basin in China is used as our laboratory working standard. More than 800 measurements including both online and offline of the compound-specific carbon isotopic compositions have been carried out by 10 laboratories (Dai et al., 2012b). International measurement standards (NBS19 and L-SVEC

$\text{CO}_2$ ) are used to perform the two-point calibrations. The carbon isotopic values were reported in  $\delta$ -notation per mil (‰) relative to VPDB. All analyses were duplicated, and the analytical precision and accuracy are better than  $\pm 0.3\text{‰}$ .

### 4 RESULTS

#### 4.1 Molecular Composition

Methane is the dominant composition, which accounts for 98.82% (average,  $n = 10$ ) in the Taiyang gas samples, 98.13% (average,  $n = 10$ ) in the Jiaoshiba gas samples, and 96.91% (average,  $n = 11$ ) in the Weirong gas samples (Table 1). The content of  $\text{C}_{2+}$  heavy hydrocarbon (mainly  $\text{C}_2\text{H}_6$  and  $\text{C}_3\text{H}_8$ ) is very small, generally less than 1%. It is 0.61% (average,  $n = 10$ ) in the Taiyang gas samples, 0.58% (average,  $n = 10$ ) in the Jiaoshiba gas samples, and 0.45% (average,  $n = 11$ ) in the Weirong gas samples. In general, Taiyang shale gas has the highest content of both methane (98.82%) and  $\text{C}_{2+3}$  heavy hydrocarbon gases (0.59%), while Weirong gas samples have the lowest content of both methane (96.91%) and  $\text{C}_{2+3}$  heavy hydrocarbon gases (0.44%). All the gases have extremely low gas wetness, which has a value of 0.21%–0.83%, indicating they belong to dry gas. The content of nonhydrocarbon gases such as  $\text{CO}_2$  and  $\text{N}_2$  is also very less (Table 1). Both the Taiyang and Jiaoshiba gases have a trace amount of  $\text{CO}_2$  and  $\text{N}_2$ , less than 1%. Weirong gas has similar content of  $\text{N}_2$  (<1%) but a relatively higher content of  $\text{CO}_2$ , in which  $\text{CO}_2$  is generally more than 1% with an average of 2.05% (average,  $n = 11$ ) and is up to 6.64% in Well Wei 43-1HF.

#### 4.2 Stable Carbon Isotopic Composition

Gas samples from the Taiyang, Jiaoshiba, and Weirong gas fields have distinct carbon isotopic values. Gases from the Taiyang gas field have the highest  $\delta^{13}\text{C}_1$  values,  $-29.5\text{‰}$  to  $-27.1\text{‰}$ , with an average of  $-28.5\text{‰}$  ( $n = 10$ ), followed by the gases from the Jiaoshiba gas field,  $-32.7\text{‰}$  to  $-29.0\text{‰}$ , with an average of  $-30.3\text{‰}$  ( $n = 10$ ), and gases from the Weirong gas field have the lowest  $\delta^{13}\text{C}_1$  values,  $-35.9\text{‰}$  to  $-34.1\text{‰}$ , with an average of  $-35.2\text{‰}$  ( $n = 11$ ) (Table 1). The carbon isotopic compositions of ethane and propane are the highest in gas samples from the Taiyang gas field ( $\delta^{13}\text{C}_2$ :  $-36.8\text{‰}$  to  $-33.7\text{‰}$ , with an average of  $-35.4\text{‰}$  ( $n = 10$ );  $\delta^{13}\text{C}_3$ :  $-37.6\text{‰}$  to  $-34.6\text{‰}$ , with an average of  $-36.2\text{‰}$  ( $n = 10$ ), followed by gas samples from Jiaoshiba gas field [ $\delta^{13}\text{C}_2$ :  $-37.5\text{‰}$  to  $-35.5\text{‰}$ , with an average of  $-36.4\text{‰}$  ( $n = 10$ );  $\delta^{13}\text{C}_3$ :  $-39.5\text{‰}$  to  $-37.7\text{‰}$ , with an average of  $-38.4\text{‰}$  ( $n = 10$ )], and are the lowest in the gas samples from Weirong gas field ( $\delta^{13}\text{C}_2$ :  $-39.7\text{‰}$  to  $-38.4\text{‰}$ , with an average of  $-38.9\text{‰}$  ( $n = 11$ );  $\delta^{13}\text{C}_3$ :  $-42.0\text{‰}$  to  $-38.7\text{‰}$ , with an average of  $-40.8\text{‰}$  ( $n = 11$ ) (Table 1).

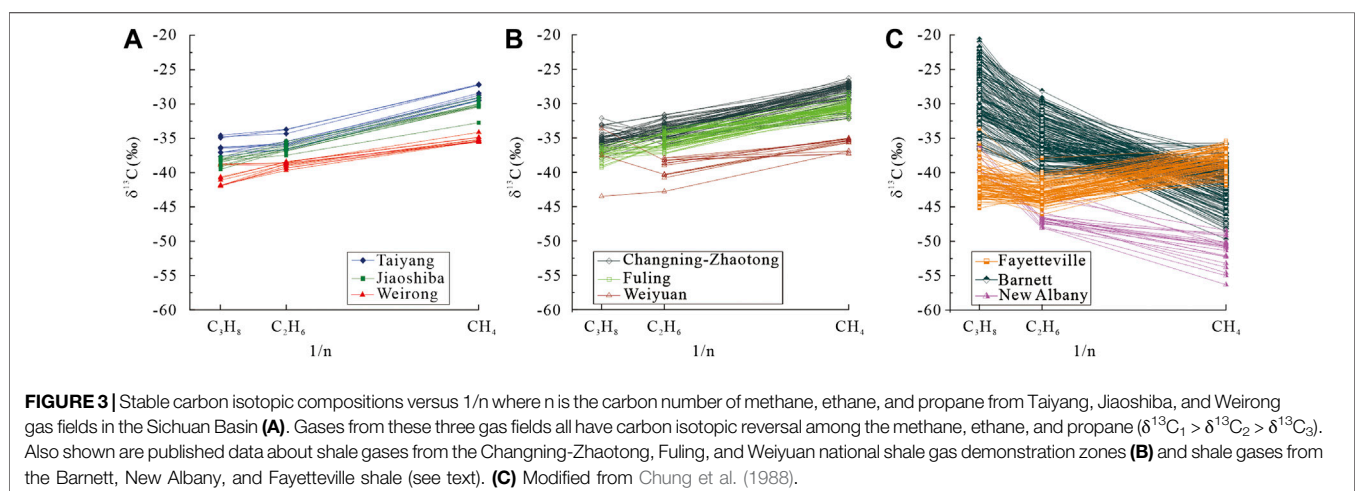
### 5 DISCUSSION

In order to further explore the gas origin, published data about shale gas from the marine facies sapropelic organic matter (Type I and II<sub>1</sub> kerogen) of the Upper Ordovician Wufeng–Lower Silurian Longmaxi shale in the Changning–Weiyuan, Fuling,

**TABLE 1** | Molecular and carbon isotopic composition of gas samples from the Upper Ordovician Wufeng–Lower Silurian Longmaxi formations in the Taiyang, Jiaoshiba, and Weirong shale gas fields in the Sichuan Basin, China.

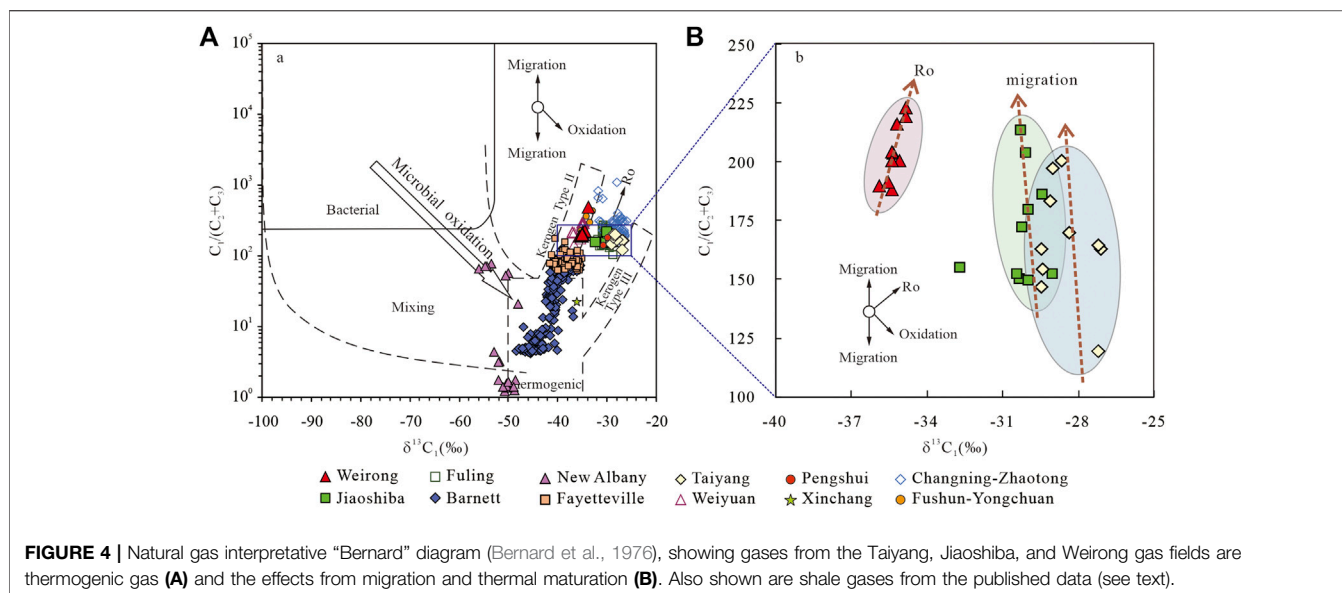
Gas field	Well	Well depth m	Burial depth m	Composition (%)					Dryness C <sub>1</sub> /C <sub>1+</sub>	δ <sup>13</sup> C (‰)		
				CH <sub>4</sub>	C <sub>2</sub> H <sub>6</sub>	C <sub>3</sub> H <sub>8</sub>	CO <sub>2</sub>	N <sub>2</sub>		CH <sub>4</sub>	C <sub>2</sub> H <sub>6</sub>	C <sub>3</sub> H <sub>8</sub>
Taiyang	Yang102 H2-2	2204.86	919.9	98.81	0.60	0.01		0.58	0.994	-29.5	-36.2	-37.0
	Yang102 H2-6	2275.24	969.95	98.88	0.63	0.01		0.48	0.994	-29.4	-36.6	-37.6
	Yang102 H2-8	2589.82	995.82	99.03	0.66	0.01		0.30	0.993	-29.5	-36.8	-37.0
	Yang105 H3-2	3,426	2245.66	98.57	0.59	0.01	0.15	0.67	0.994	-27.1	-33.7	-34.9
	Yang105 H3-4	3,390	2140.76	98.88	0.59	0.01	0.14	0.37	0.994	-27.2	-33.7	-34.6
	Yang105 H3-6	3,325	2059.13	98.50	0.71	0.11	0.13	0.41	0.992	-27.2	-34.3	-34.8
	Yang105 H2-2	2,300	1544.28	98.94	0.57	0.02	0.05	0.40	0.994	-28.4	-35.7	-36.3
	Yang105 H2-4	2,400	1501.065	98.88	0.53	0.01	0.05	0.52	0.995	-29.1	-35.9	-36.3
	Yang105 H2-6	2,285	1414.845	98.76	0.49	0.01		0.45	0.995	-29.1	-35.4	-37.1
	Yang105 H2-8	2,300	1249.86	99.01	0.48	0.01		0.50	0.995	-28.7	-36.0	-36.5
Jiaoshiba	JY1-2HF	4,168	2416.215	98.09	0.62	0.03	0.31	0.84	0.993	-30.3	-35.5	-37.7
	JY2-3HF	4,518	2479.58	98.23	0.63	0.02	0.31	0.81	0.993	-29.0	-35.7	-38.1
	JY3-3HF	3,561	2428.855	97.98	0.61	0.02	0.35	0.95	0.994	-32.7	-37.5	-38.2
	JY4-2HF	4,312	2598.44	98.21	0.56	0.01	0.44	0.77	0.994	-30.2	-36.5	-38.2
	JY56-2HF	4,498	2818.265	98.09	0.52	0.01	0.57	0.81	0.995	-29.4	-36.1	-38.0
	JY18-5HF	4,650	2820.685	98.14	0.53	0.02	0.34	0.96	0.994	-30.0	-36.5	-38.9
	JY9-6HF	4,147	2310.17	98.26	0.64	0.02	0.21	0.87	0.993	-30.0	-36.2	-38.5
	JY39-7HF	5,410	2778.295	98.18	0.63	0.02	0.37	0.81	0.993	-30.4	-36.8	-39.5
	JY37-6HF	5,865	3139.72	98.09	0.47	0.01	0.60	0.83	0.995	-30.1	-36.6	-39.2
	JY61-2HF	4,770	3037.515	98.01	0.45	0.01	0.66	0.88	0.995	-30.3	-36.9	-38.1
Weirong	WY29-1HF	5,430	3,743	97.66	0.46	0.02	1.26	0.60	0.995	-35.4	-39.3	-41.9
	WY29-2HF	5,390	3,737	97.70	0.50	0.02	1.20	0.58	0.995	-35.9	-39.3	-42.0
	WY29-4 + 5 + 6		3,690	97.76	0.50	0.02	1.19	0.52	0.995	-35.4	-39.7	-41.8
	WY23-4HF	5,546	3,800	97.42	0.44	0.02	1.64	0.49	0.995	-35.2	-38.8	-41.1
	WY23-2HF	5,600	3830.22	97.23	0.42	0.01	1.72	0.61	0.996	-34.9	-38.4	-40.8
	WY23-6HF	5,596	3831.96	97.41	0.43	0.01	1.66	0.48	0.995	-34.9	-38.5	-40.7
	WY43-1HF	5,520	3,720	91.91	0.19	0.00	6.64	1.25	0.998	-34.1	-38.6	-38.8
	WY43-2HF	5,540	3,737	96.37	0.46	0.02	2.76	0.38	0.995	-35.1	-38.9	-38.9
	WY43-3HF	5,585	3,744	97.40	0.48	0.03	1.59	0.49	0.995	-35.6	-38.6	-38.7
	WY43-4HF	5,595	3,778	97.55	0.46	0.02	1.53	0.44	0.995	-35.4	-38.7	-41.9
WY43-5HF	5,610	3,770	97.58	0.47	0.02	1.38	0.55	0.995	-35.4	-39.1	-42.0	

Note: All the wells are horizontal and comprise vertical and horizontal portions. Well depth represents the depth including the actual vertical portion and the horizontal portion. Burial depth represents the actual vertical portion.



and Zhaotong national shale gas demonstration zones, Pengshui and Yongchuan area in the Sichuan Basin, shale gas from the marine facies sapropelic organic matter of the Barnett shale in the

Fort Worth Basin, Fayetteville shale in the Arkoma Basin, and New Albany shale in the Illinois Basin were also investigated (Cao et al., 2020; Chen et al., 2020; Dai et al., 2016b; Feng et al., 2019;



Feng et al., 2020; Feng et al., 2016; Lin et al., 2017; Wei et al., 2016; Wu et al., 2015; Zhang et al., 2018a; Martini et al., 2008; Rodriguez and Philp, 2010; Strąpoć et al., 2010; Zumberge et al., 2012).

## 5.1 Origin of the Gas

Carbon isotopic reversal occurs widely among the  $C_1$ – $C_3$  n-alkanes, that is, methane and its homologs get more depleted in  $^{13}C$  with increasing carbon number ( $\delta^{13}C_1 > \delta^{13}C_2 > \delta^{13}C_3$ ) (Figure 3A; Table 1). In general, this is consistent with previous studies of the shale gases from the Changning–Zhaotong, Weiyuan, and Fuling national shale gas demonstration zones (Figure 3B). In contrast, gas samples from the Barnett and New Albany shales mostly have a positive carbon isotopic distribution pattern among the  $C_1$ – $C_3$  alkane gases ( $\delta^{13}C_1 < \delta^{13}C_2 < \delta^{13}C_3$ ), and those from the Fayetteville shale have similar carbon isotopic reversal (Figure 3C) (Martini et al., 2008; Rodriguez and Philp, 2010; Strąpoć et al., 2010; Zumberge et al., 2012).

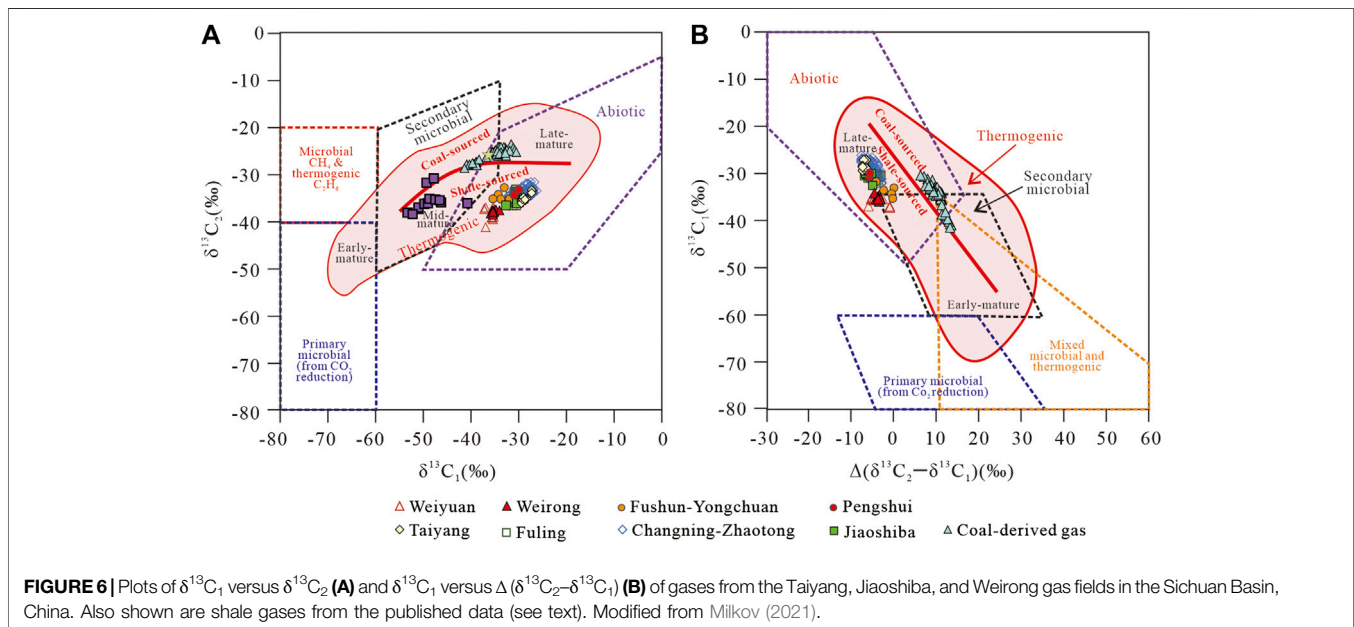
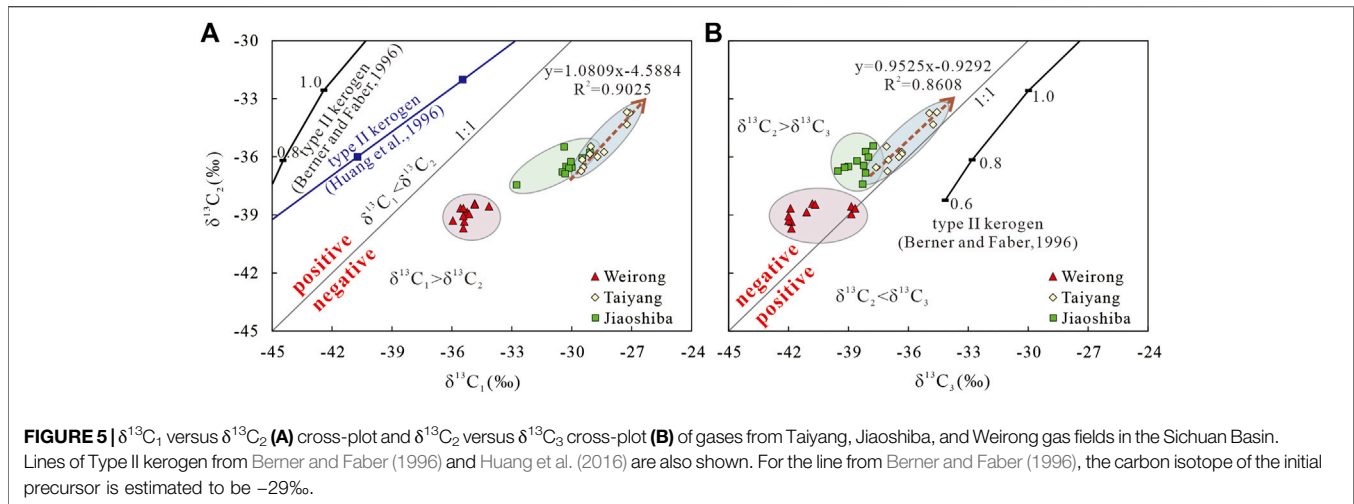
Numerical studies have suggested a cut-off  $\delta^{13}C_2$  value of  $-28\text{‰}$  to distinguish the gases sourced from humic and sapropelic organic matter, that is, gases sourced from humic organic matter have  $\delta^{13}C_2 > -28\text{‰}$ , while gases sourced from sapropelic organic matter have  $\delta^{13}C_2 < -28\text{‰}$  (Chen et al., 1995; Dai et al., 2009; Dai et al., 2012a; Dai et al., 2014b; Liang et al., 2002; Ni et al., 2014; Ni et al., 2015; Ni et al., 2019b). Gases from Taiyang, Jiaoshiba, and Weirong gas fields have  $\delta^{13}C_2 < -33\text{‰}$ , and should source from sapropelic organic matter according to the criterion of  $\delta^{13}C_2$  value. However, such a distinguishing criterion is effective for gases with normal carbon isotopic distribution patterns which have not undergone secondary alteration but may not be applicable for gases with carbon isotopic reversal (Dai et al., 2013). Therefore, genetic information should be obtained from indexes and not only the  $\delta^{13}C_2$  values.

“Bernard diagram,” based on the carbon isotopic value of methane and the molecular composition of methane and ethane, was often used to determine the gas origin and later modifications (Bernard et al., 1976). This diagram differentiates the

thermogenic and bacterial gases and shows the type of kerogen and later secondary alterations such as mixing between thermogenic and bacterial gases, migration, oxidation, and thermal maturation. Except gases from the New Albany in the Illinois Basin that have mixing effects, all other gases fall in the thermogenic gas area and have no impacts from bacterial gas (Figure 4A). Figure 4B demonstrates that gases from the Weirong gas field are mainly affected by the thermal maturation, but gases from the Jiaoshiba and Taiyang gas fields are likely affected by the migration effects.

In the  $\delta^{13}C_1$  versus  $\delta^{13}C_2$  and  $\delta^{13}C_2$  versus  $\delta^{13}C_3$  cross-plots, in general, the least mature gases lie in the lower left area and most mature gases lie in the upper right area. Theoretically, gases which have not undergone secondary alteration and are from the same source rocks but with different thermal maturation stages will lie on a straight line. Gases from the Taiyang, Jiaoshiba, and Weirong shale gas fields fall on the bottom right side of the diagram close to the area of sapropelic Type II kerogen and also in the area below the 1:1 line of  $\delta^{13}C_1$  versus  $\delta^{13}C_2$  (Figure 5A). This indicates gases from the Taiyang, Jiaoshiba, and Weirong gas fields were sourced from sapropelic organic matter. Figure 5A also shows a very low carbon isotopic composition of ethane, therefore demonstrating a carbon isotopic reversal between methane and ethane ( $\delta^{13}C_1 > \delta^{13}C_2$ ). Similarly, in the plot of  $\delta^{13}C_2$  versus  $\delta^{13}C_3$ , gases from the three gas fields fall in the area close to that of the sapropelic Type II kerogen (Berner and Faber, 1996) and demonstrate a carbon isotopic reversal between ethane and propane ( $\delta^{13}C_2 > \delta^{13}C_3$ ) (Figure 5B).

Recently, new diagrams of  $\delta^{13}C_1$  versus  $\delta^{13}C_2$  and  $\delta^{13}C_1$  versus  $\Delta$  ( $\delta^{13}C_2 - \delta^{13}C_1$ ) were proposed to separate the shale-sourced and coal-sourced gases (Milkov, 2021). Both the  $\delta^{13}C_1$  versus  $\delta^{13}C_2$  and  $\delta^{13}C_1$  versus  $\Delta$  ( $\delta^{13}C_2 - \delta^{13}C_1$ ) diagrams can distinguish gases of primary microbial, secondary microbial, thermogenic, and abiogenic origins, and the thermogenic gas includes mid-mature to late-mature shale-sourced and coal-sourced gases (Figure 6). Gases from the marine facies Taiyang, Jiaoshiba, and Weirong gas

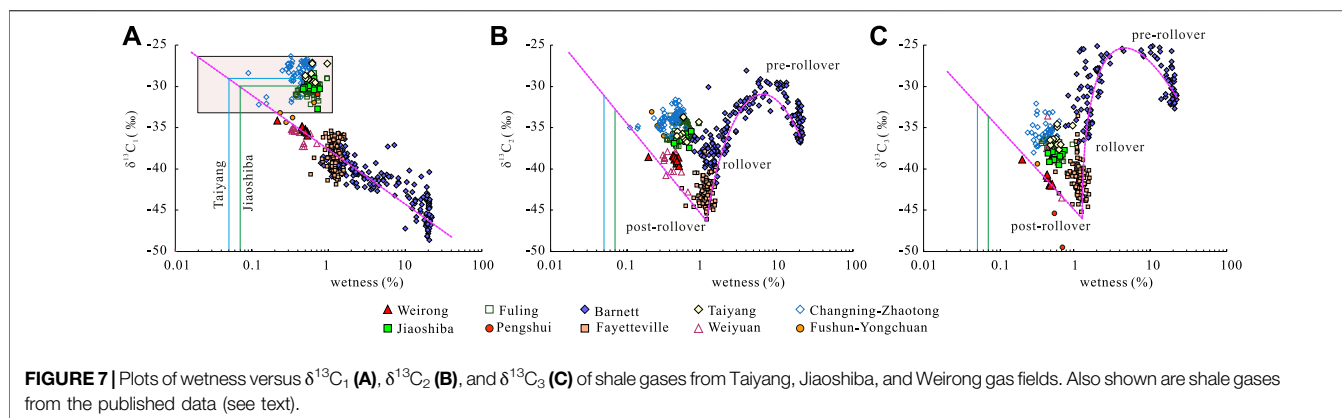


fields fall in the area of shale-sourced thermogenic gas toward the late-mature thermal evolution stage, which is similar to the shale gases from the Weiyuan, Fuling, Changning–Zhaotong, Pengshui, and Yongchuan areas. Among the nine sets of source rocks in the Sichuan Basin, source rocks above the Wufeng–Longmaxi shale are impossible to have a contribution. The Qixia and Maokou source rocks are a set of carbonate deposits, the Longtan and Xujiache source rocks are a set of coal measure deposit, and the Dalong source rocks are locally distributed in northern Sichuan. The Sinian source rocks are mainly distributed in the margins of the Basin and have little contribution. Though the Qiongzhusi shale is widely distributed, the Ordovician deposit is very thick, and the thickness can be up to 600 m. The hot shale in the Wufeng–Longmaxi formations is generally less than 50 m and concentrated in the Wufeng and the

Lower Longmaxi formations. Hence, gases in the Taiyang, Jiaoshiba, and Weirong shale gas fields are shale gas reservoirs and sourced in the Wufeng–Longmaxi shale.

## 5.2 Carbon Isotope of Methane

When plotting the  $\delta^{13}\text{C}_1$  versus gas wetness, gases from Weirong, Weiyuan, Barnett, and Fayetteville have a good linear relationship, while gases from Taiyang and Jiaoshiba are characterized by an enrichment of  $^{13}\text{C}$  in methane and thus shift away from the linear maturity trend (Figure 7A). The  $^{13}\text{C}$ -enriched methane was considered to be a late-stage methane and result from Rayleigh-type isotopic fractionation of ethane (Feng et al., 2020); however, such a mechanism may not satisfy the mass and isotopic balance requirements (Xia and Gao, 2018). In the southern Sichuan Basin, geological conditions are



more complex than those in the Appalachian Basin. The Wufeng–Longmaxi shale has experienced very high geotemperature and is at the over-mature stage at present and has suffered extensive uplifts locally. Considering these complex conditions, more influences should be considered in the southern Sichuan Basin. The offset of the  $\delta^{13}\text{C}_1$  values in Taiyang and Jiaoshiba shale gas fields could be caused either by enrichment of  $^{13}\text{C}$  in methane or by an increase in wetness. Compared to the Cambrian and Sinian conventional natural gas in the Weiyuan gas field ( $-32.7\text{‰}$  to  $32.0\text{‰}$ ) (Dai, 2003; Wu et al., 2014), the Silurian Wufeng–Longmaxi shale gas in Taiyang and Jiaoshiba areas is clearly more enriched in  $^{13}\text{C}$ .

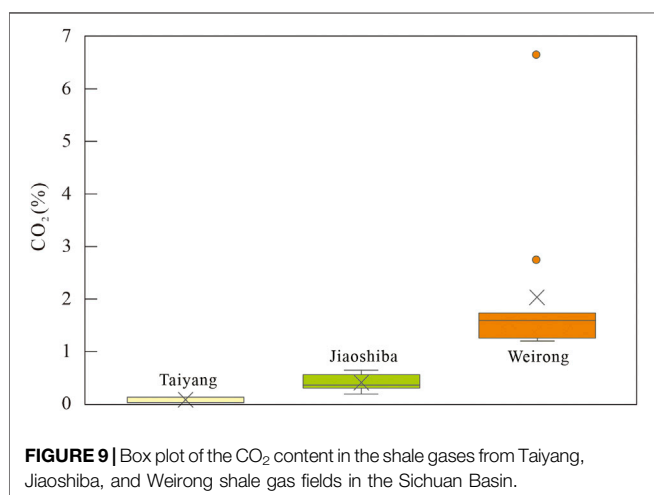
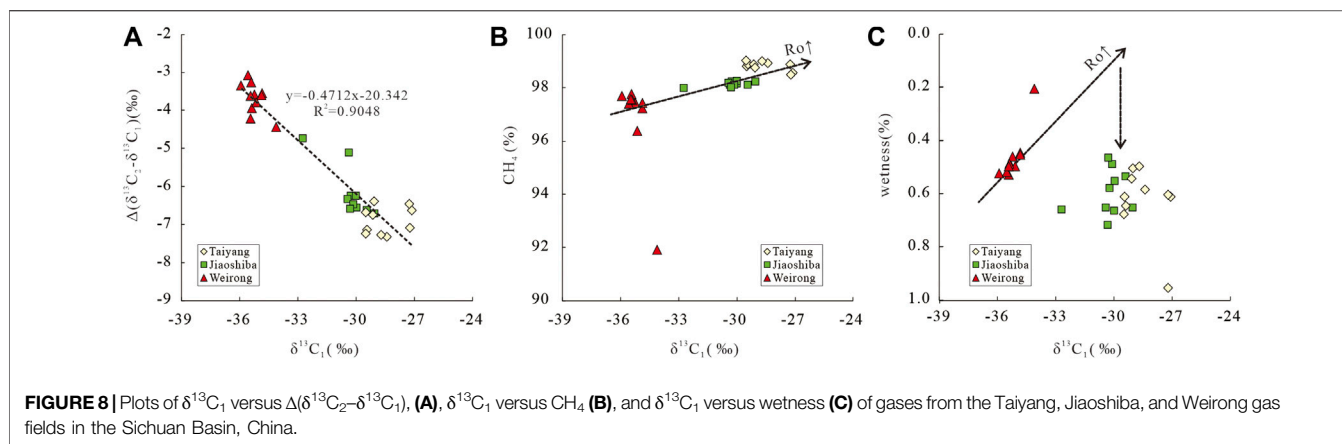
### 5.2.1 Thermal Maturity of the Source Rocks

Various models have demonstrated the linear logarithmic relationship between the carbon isotopic composition of methane and the thermal maturity (Ro%) of source organic matter (Stahl and Carey, 1975; Schoell, 1980; Dai and Qi, 1989; Berner and Faber, 1996). In the oil window, methane is primarily generated from kerogen cracking. When thermal maturity still increases, wet gas cracking begins, which will increase methane but decrease in gas wetness (Prinzhofer and Huc, 1995). Hence, the carbon isotope of methane generally increases with increasing thermal maturity of the source rocks, and methane generated at higher thermal maturity normally has a higher carbon isotope and lower gas wetness.

Though the Wufeng–Longmaxi shale in the southern Sichuan Basin is generally all at the over-mature stage, differences still exist in different areas. Shale in the Weiyuan area has a relatively low equivalent Ro% of 2.25% (1.8%–2.7%) (Wang et al., 2019; Zou et al., 2021); correspondingly, its shale gas has the lowest  $\delta^{13}\text{C}_1$  values (average =  $-35.2\text{‰}$ ) and wetness of 0.47% (0.21%–0.53%), which falls on the linear maturity trend. Shale in the Taiyang area has the highest equivalent Ro% of 3.45% (3.0%–3.9%) (Wang et al., 2019; Liang et al., 2020a; Liang et al., 2020b; Zou et al., 2021); correspondingly, its shale gas has the highest  $\delta^{13}\text{C}_1$  values (average =  $-28.5\text{‰}$ ) and wetness of 0.61% (0.50%–0.83%), which falls off the linear maturity trend. Compared to the Weirong shale gas, the Taiyang shale gas should have lower gas wetness due to its higher thermal maturity. Similarly, shale in the Jiaoshiba area has an

equivalent Ro% of 3.1% (2.6%–3.6%) (Dai et al., 2014a; Wang et al., 2019; Zou et al., 2021), which is higher than that in Weirong but lower than that in Taiyang. Correspondingly, its shale gas also has  $\delta^{13}\text{C}_1$  values (average =  $-30.3\text{‰}$ ) higher than those that in Weirong but lower than those in Taiyang, and gas wetness of 0.59% (0.47%–0.67%), which also falls off the linear trend line (Figure 7A). Compared to the Weirong shale gas, the Jiaoshiba shale gas also should have lower gas wetness due to its higher thermal maturity. As shown in Figure 7A, if thermal maturity is the controlling factor, the Taiyang shale gas should have gas wetness around 0.05%, while the Jiaoshiba shale gas should have gas wetness around 0.07%, which is an order of magnitude lower than the actual determined wetness. According to such low gas wetness, the carbon isotopes of ethane and propane are relatively lower than expected (Figures 7B, C).

Carbon isotopic differences between methane and ethane [ $\Delta(\delta^{13}\text{C}_2 - \delta^{13}\text{C}_1)$ ] have been used to reflect the maturity influences on gases. As thermal maturity increases, the isotopic differences between methane and ethane decreases; therefore, the more mature gases normally will have smaller  $\Delta(\delta^{13}\text{C}_2 - \delta^{13}\text{C}_1)$  values (James, 1983; Clayton, 1991; Tang et al., 2000). Shale gases from Taiyang, Jiaoshiba, and Weirong gas fields generally demonstrate a good linear inverted relationship between the  $\delta^{13}\text{C}_1$  value and  $\Delta(\delta^{13}\text{C}_2 - \delta^{13}\text{C}_1)$  value ( $R^2 = 0.9048$ ). The  $\delta^{13}\text{C}_1$  value increases from  $-36\text{‰}$  to  $-27\text{‰}$ , correspondingly, and the  $\Delta(\delta^{13}\text{C}_2 - \delta^{13}\text{C}_1)$  value changes from  $-3\text{‰}$  to  $-8\text{‰}$  (Figure 8A). The carbon isotopic differences between methane and ethane get larger with increasing thermal maturity, which is opposite to the normal trend (Figure 8A). This is mainly caused by the depletion of  $^{13}\text{C}$  in ethane with increasing thermal maturity. As the thermal maturity increases, methane becomes more enriched at  $^{13}\text{C}$ , while ethane gets more depleted at  $^{13}\text{C}$ ; hence, the higher the thermal maturity, the larger the  $\delta^{13}\text{C}$  differences between methane and ethane. This linear correlation implies that thermal maturity should be the controlling factor on the carbon isotopes of the shale gas. In addition to the thermal maturity of the source rocks, there should be a process that will increase the amount of wet gas but will not significantly impact the amount of methane (Figures 8B, C). As shown in Figure 8, methane content generally increases with increasing  $\delta^{13}\text{C}_1$  values in the three gas fields, while shale gas in



the Taiyang and Jiaoshiba gas fields apparently has higher wet gas.

### 5.2.2 Fischer-Tropsch-Type Synthesis of Hydrocarbon

Fischer-Tropsch-type synthesis of hydrocarbon from  $\text{CO}_2$  and  $\text{H}_2$  may have contributed to the increasing amount of wet gas and depletion of  $^{13}\text{C}$  in hydrocarbon gas. The  $\text{CO}_2$  content varies apparently in the Taiyang, Jiaoshiba, and Weirong shale gas fields. The  $\text{CO}_2$  content is highest in the Weirong shale gas field, 1.19%–6.64% (average = 2.05%); followed by the Fuling shale gas field, 0.21%–0.66% (average = 0.42%); and the lowest in the Taiyang shale gas field, 0.05%–0.15% (average = 0.10%) (Figure 9). Among the 10 gas samples in Taiyang,  $\text{CO}_2$  is detected only in five samples. From the Weirong gas field to the Taiyang gas field, the equivalent  $\text{Ro}\%$  increases from 2.25% to 3.45% (Wang et al., 2019; Liang et al., 2021; Zou et al., 2021), while the  $\text{CO}_2$  content decreases from 2.05% to 0.10%. The carbon isotope of  $\text{CO}_2$  in the Jiaoshiba area varies from  $-5.8\text{‰}$  to  $10.4\text{‰}$  (average =  $3.7\text{‰}$ ) (Feng et al., 2020), which was considered to be the product of thermal metamorphism of carbonate minerals (Dai et al., 2022). Carbonate minerals are abundant in the Wufeng-Longmaxi shale (Dai et al., 2014a; Dai

et al., 2016b), and with increasing thermal maturity, thermal metamorphism will generate more  $\text{CO}_2$ . There must be a sink for  $\text{CO}_2$  with increasing thermal maturity in the Jiaoshiba and Taiyang areas.

During the late cantagensis stage, water is likely involved in the generation of methane (Burruss and Laughrey, 2010). A Fischer-Tropsch-type synthesis of hydrocarbon from  $\text{CO}_2$  and  $\text{H}_2$  is expected to occur through the following two equations:  $\text{CH}_x$  (organic matter) +  $2\text{H}_2\text{O} \rightarrow \text{CO}_2 + (2 + x/2) \text{H}_2$  and  $\text{CO}_2 + m\text{H}_2 \rightarrow x\text{CH}_4 + y\text{C}_2\text{H}_6 + \dots + z\text{H}_2\text{O}$  (Tang and Xia, 2011). Among them,  $\text{CO}_2$  could be from the thermal metamorphism of carbonate minerals in the shale and also from the water reforming reaction of organic matter. Higher thermal maturity represents longer reaction time and more consumption of  $\text{CO}_2$  in the system, so the  $\text{CO}_2$  content is the most in the Weirong shale gas field and the least in the Taiyang shale gas field. Such Fischer-Tropsch-type synthesis of hydrocarbon from  $\text{CO}_2$  and  $\text{H}_2$  has also been reported in the pyrolytic experiments of shale (Gao et al., 2014) and coal samples (Gao et al., 2018), and apparent carbon isotopic depletion in gaseous products has been documented.

With continuous cracking of wet gas, the amount of wet gas (mainly  $\text{C}_2 + \text{C}_3$ ) will decrease, that is, the ethane content is less than 0.5% for Weirong shale gas. Due to the amount of  $\text{CO}_2$  and  $\text{H}_2$ , the number of hydrocarbon gases generated *via* Fischer-Tropsch-type synthesis should be minimal. Hence, limited mixing between the late stage shale gas with the Fischer-Tropsch-type synthesized gas will significantly increase the wet gas content but have little impact on the methane content; similarly, the carbon isotopic depletion impact is little on methane, but to some extent significant on ethane and propane. This should be part of the reasons causing the isotopic depletion in ethane and propane.

### 5.2.3 $\delta^{13}\text{C}$ Value of the Source Organic Matter

In the southern Sichuan Basin, the  $\delta^{13}\text{C}$  value of source organic matter may also have influenced on the  $\delta^{13}\text{C}$  value of hydrocarbon gases. Generally, higher  $\delta^{13}\text{C}$  values of source rocks correspond to higher  $\delta^{13}\text{C}$  values of gases generated

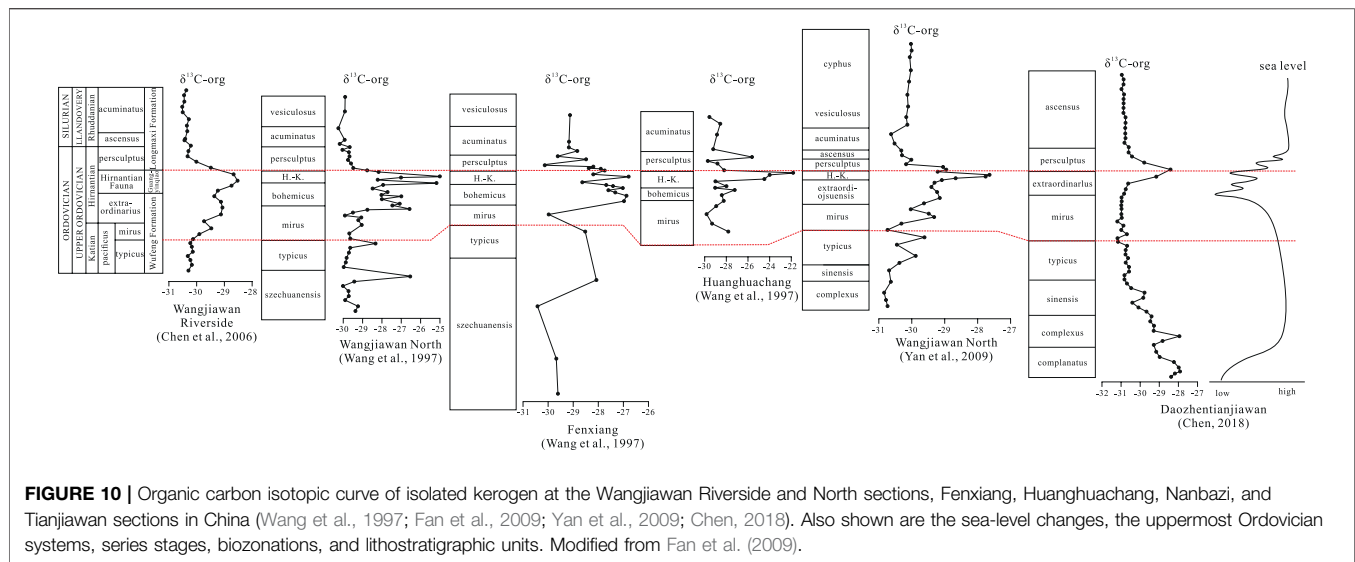


**FIGURE 10 |** Organic carbon isotopic curve of isolated kerogen at the Wangjiawan Riverside and North sections, Fenxiang, Huanghuachang, Nanbazi, and Tianjiawan sections in China (Wang et al., 1997; Fan et al., 2009; Yan et al., 2009; Chen, 2018). Also shown are the sea-level changes, the uppermost Ordovician systems, series stages, biozonations, and lithostratigraphic units. Modified from Fan et al. (2009).

from them, which is the inheritance effect of the carbon isotope (Dai et al., 1992).

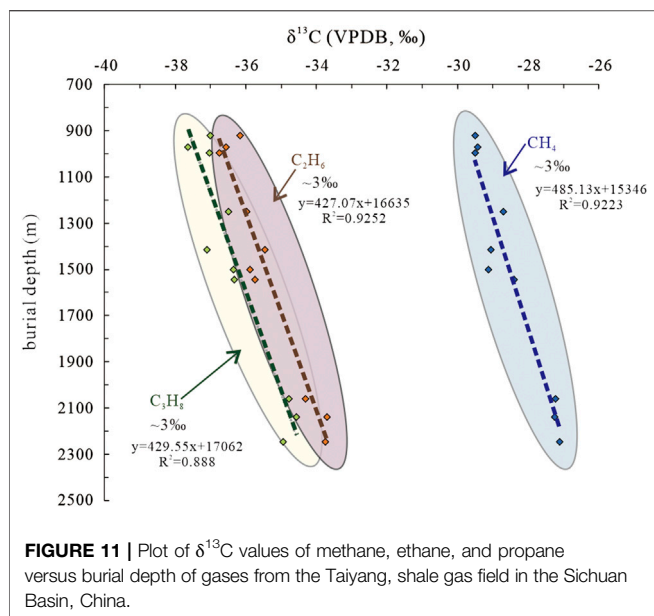
A prominent positive carbon isotopic excursion of both shale and limestones has been recorded in the Late Ordovician Hirnantian stage (Middle and Upper Wufeng Formation in Sichuan Basin) in North America (Bergström et al., 2006; Orth et al., 1986), Europe (Brenchley et al., 1994; Marshall et al., 1997), and China (Figure 10) (Chen, 2018; Fan et al., 2009; Wang et al., 1993; Wang et al., 1997), which has been regarded as to be associated with the Gondwana glaciation. The positive carbon isotopic excursion is up to 5‰–7‰ in the Hirnantian limestones (Qing and Veizer, 1994; Marshall et al., 1997; Kump et al., 1999) and is up to –21.1‰ in the Tianjiawan shale in Daozhen county and –26.6‰ in the Nanbazi shale in Tongzi county (Chen, 2018). In addition to the positive carbon isotopic excursion of the organic matter during the Hirnantian stage, several studies have also demonstrated a significant positive carbon isotopic excursion (~8‰) of the organic matter in the early Katian (Lower Wufeng Formation in Sichuan Basin) or the Guttenberg stage in the late Middle Ordovician, which was caused by the decrease in surface-water CO<sub>2</sub> concentrations and the enrichment of microfossil *Gloeocapsomorpha Prisca* (Jacobson et al., 1988; Pancost et al., 1999; Pancost et al., 2013). Compounds exclusively from *Gloeocapsomorpha Prisca* may contribute a positive carbon isotopic shift of 3.5‰, indicating the significant contribution from source organic matter (Pancost et al., 2013). The δ<sup>13</sup>C of shale decreased in the Rhuddanian stage (Lower Longmaxi Formation). Actually, the δ<sup>13</sup>C value of kerogen is about –31.0‰ to –27.8‰ in the Changning–Zhaotong areas, –29.9‰ to –28.6‰ in the Jiaoshiba area (Lin et al., 2017), and –36.0‰ to –27.9‰ in the Weiyuan areas (Feng et al., 2018).

Gases sourced from the Wufeng shale are expected to be enriched in <sup>13</sup>C due to the positive carbon isotopic excursion. The continuous sedimentation and thin thickness of Wufeng–Longmaxi hot shale indicate that post-genetic

processes such as migration and mixing in the shale layers are possible and contribution from the <sup>13</sup>C-enriched Wufeng shale cannot be ignored. The “sweet spot” of the Wufeng–Longmaxi shale gas is mainly concentrated in the Wufeng Formation and the lower part of the Longmaxi Formation, with a thickness of 15–50 m, and the Rhuddanian stage is the prime stage of the development of the Lower Silurian organic-enriched shale and also the key stage for the formation of “sweet spot” of shale gas (Zou et al., 2016; Zou et al., 2019). According to the graptolite occurrence, sedimentation from the Late Ordovician to the Early Silurian is continuous (Liang et al., 2018; Liang et al., 2020a; Rong et al., 2011; Rong et al., 2019). Particularly, in the Taiyang area, shale with TOC > 1% has a thickness of 50.3–57.0 m, and it is characterized by longitudinal continuous distribution without an interlayer in the middle (Liang et al., 2020b). Diffusive migration has been found in the Jiaoshiba area, where δ<sup>13</sup>C<sub>1</sub> values increased with proximity to the fault zone (Feng et al., 2020). In the Taiyang shale gas field, the linear relationship between burial depth and δ<sup>13</sup>C values of methane, ethane, and propane also indicates possible influences from gas migration. However, the contribution from the carbon isotope of source organic matter cannot be the controlling factor on the enrichment of <sup>13</sup>C in methane. Though the Taiyang shale gas field is close to the Qianzhong paleo-uplift and located on the southern slope of the depression, the sea-level fall in the Hirnantian stage was significant, the positive carbon isotopic excursion should also be important, and TOC could even be up to 8%, while the thickness of the Hirnantian deposit is small, generally 2–3 m, so the contribution from the precursor organic matter should not be ignored but cannot be controlling.

#### 5.2.4 Diffusion and Adsorption/Desorption

Shale gas from the Taiyang gas field shows a good linear correlation between δ<sup>13</sup>C<sub>1</sub> and δ<sup>13</sup>C<sub>2</sub> (R<sup>2</sup> = 0.9025) and between δ<sup>13</sup>C<sub>2</sub> and δ<sup>13</sup>C<sub>3</sub> (R<sup>2</sup> = 0.8608) (Figure 5). Such good



linear correlation is not necessarily caused by thermal maturity. When plotting the carbon isotope of shale gas from the Taiyang gas field versus their actual vertical burial depth, it is clear that methane, ethane, and propane become more enriched in  $^{13}\text{C}$ , with increasing burial depth. When the burial depth changes from  $\sim 2300$  to  $\sim 900$  m, the carbon isotopic composition of methane, ethane, and propane all decreases by about  $\sim 3\text{‰}$ , and a linear correlation of such carbon isotopic changes exists for methane ( $R^2 = 0.9223$ ), ethane ( $R^2 = 0.9252$ ), and propane ( $R^2 = 0.888$ ) (Figure 11). Due to the geothermal gradient, increasing burial depth usually represents the increase of geo-temperature and thus thermal maturity; hence,  $\delta^{13}\text{C}$  values of hydrocarbon gases usually increase with increasing burial depth. However, the Wufeng–Longmaxi shale in the Taiyang area underwent deep burial from Triassic to Jurassic, resulting in the high thermal maturity, and began to uplift in the Cretaceous, so deep burial does not necessarily mean high geo-temperature and shale with different burial depths may have very similar thermal maturity. For example, the Longmaxi shale in Well Y109 has a burial depth of 2162–2202 m and equivalent Ro% of 3.1%, while the Longmaxi shale in Well Y102 has a much shallower burial depth (732–741 m) but still has similar equivalent Ro% (3.0%) (Liang et al., 2021). Therefore, there must be other post-genetic processes that cause the linear correlation between the burial depth and  $\delta^{13}\text{C}$  values of hydrocarbon gases. Though the Wufeng–Longmaxi shale in the Taiyang area is typically characterized by shallow burial depth (can be less than 1,000 m), diffusive gas leakage might occur in these shallow layers. In the Taiyang area, the decreasing carbon isotopic compositions of hydrocarbon gas with decreasing burial depth cannot be caused by diffusive gas leakage. In general, diffusive gas leakage is more likely to occur in shallow layers. During the leakage, since  $^{12}\text{C}$ - $^{12}\text{C}$  bonds are weaker than  $^{12}\text{C}$ - $^{13}\text{C}$  bonds and leak faster, the leaking gas will be more enriched in methane and depleted in  $^{13}\text{C}$ , and the residual gas which is still trapped in the

reservoir will be more depleted in methane but enriched in  $^{13}\text{C}$ . If gas leakage occurs in the shallow layers, gases in the shallow layers will be more enriched in  $^{13}\text{C}$  compared to those of the deep layers. Apparently, this is opposite to the case in the Taiyang shale gas field.

Carbon isotopic fractionation of methane due to mass transport has been evaluated in many studies, especially in low-permeability shale. During gas transport,  $^{12}\text{C}$ - $^{12}\text{C}$  bonds are weaker than  $^{12}\text{C}$ - $^{13}\text{C}$  bonds and transport faster; thus, it caused a significant isotopically lighter carbon than the source (Pernaton et al., 1996; Zhang and Krooss, 2001). Previous studies documented a large isotopic fractionation during gas migration under a nonsteady state (Prinzhofer and Pernaton, 1997; Zhang and Krooss, 2001). Zhang and Krooss (2001) proposed that the magnitude of depletion in  $^{13}\text{C}$  is the highest during the initial nonsteady state of the diffusion process and decreases to a constant difference when it approached the steady state. Canister desorption experimental study about the Longmaxi shale samples at reservoir temperatures showed a rapid enrichment of  $^{13}\text{C}$  up to 13.7‰–16.2‰ in methane as desorption proceeds (Ma et al., 2020). Li et al. (2020) proposed to divide the gas transport process during a complete production into four stages and demonstrated that methane became depleted in  $^{13}\text{C}$  during the transition stage (stage II) and became enriched in  $^{13}\text{C}$  during the adsorbed gas desorption stage (stage III), while became depleted in  $^{13}\text{C}$  again during the diffusion stage (stage IV). Carbon isotopic enrichment of methane due to adsorption/desorption during stage IV might contribute to the heavy carbon isotope of methane in Taiyang and Jiaoshiba shale gas fields. However, according to the analytical results and numerical calculations, it is suggested that under geological conditions, post-genetic coupled diffusion and adsorption/desorption due to gas transport normally cause isotopic fractionation of less than 5‰ (Xia and Tang, 2012). In the Taiyang shale gas field, once diffusive migration occurs, the separates will be more enriched in methane and depleted in  $^{13}\text{C}$ , resulting in the relatively low  $\delta^{13}\text{C}$  values in the shallow layer, while the residual will be more depleted in methane and enriched in  $^{13}\text{C}$ , resulting in the relatively high  $\delta^{13}\text{C}$  values in the deep layer. The  $\text{C}_1/(\text{C}_2+\text{C}_3)\sim\delta^{13}\text{C}_1$  plot also shows that the Taiyang shale gas has a rapid change in molecular composition with burial depth, indicating potential effects from diffusive migration (Figure 11).

The geological conditions of the Taiyang gas field also support possible diffusive gas migration in this area. The main part of the Taiyang shale gas field is the Taiyang anticline, with a gas-bearing area of 580 km<sup>2</sup>. It has suffered alteration from the superimposed multistage tectonic activities since the Caledonian period. The Taiyang anticline is characterized by “strong superimposed fold deformation and weak multistage fault reconstruction,” and develops nearly east–west reverse faults and nearly south–north strike–slip faults. The nearly east–west faults are developed on the top and two wings of the anticline due to the north–south compression stress in the early stage. With continuous compression stress from north–south, the complex anticline gradually deforms and forms nearly north–south strike–slip faults. The uplift and denudation stage of extrusion

strike-slip in the Late Yanshanian-Himalayan period resulted in the shallow burial depth of Wufeng–Longmaxi formations, that is, 500–1,500 m in the main part of the anticlinal structure (Liang et al., 2021). The formation pressure coefficient is 1.22–1.47, natural micro-cracks are developed in the shale, and the porosity is 4%–9%, with an average of 5.67% (Liang et al., 2020a). Therefore, diffusive migration of shale gases is likely to occur during or after the uplift and denudation stages.

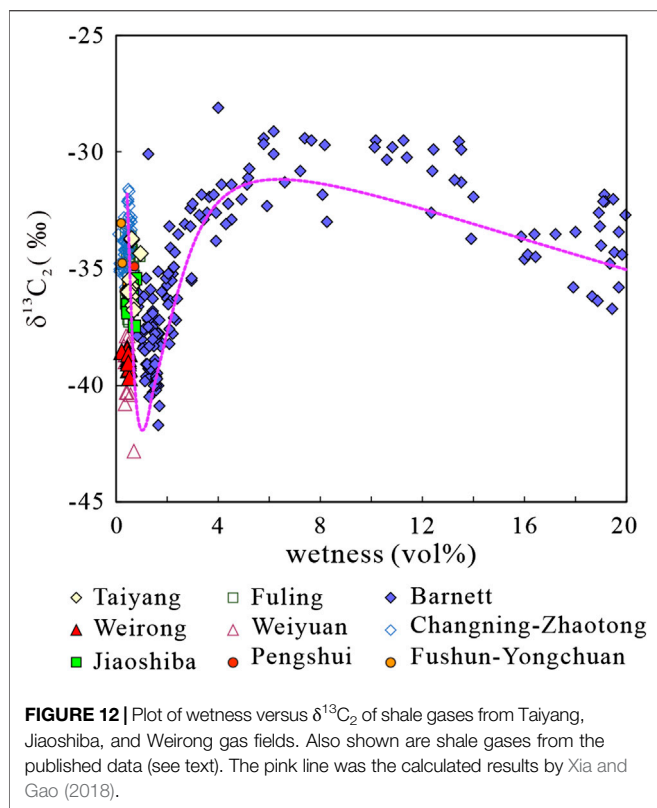
### 5.3 Depletion of $^{13}\text{C}$ in Ethane and Propane

At low mature and mature stages,  $\delta^{13}\text{C}$  values of  $\text{CH}_4$  are much lower than those of  $\text{C}_2\text{H}_6$  and  $\delta^{13}\text{C}$  values of  $\text{C}_2\text{H}_6$  are much lower than those of  $\text{C}_3\text{H}_8$ , that is,  $\delta^{13}\text{C}_1 > \delta^{13}\text{C}_2 > \delta^{13}\text{C}_3$ . When the source rocks reach the oil window with Ro% of 1.5%, the carbon isotopic difference between methane and ethane and between ethane and propane will approach a similar value of  $-6\text{‰}$  (Cesar et al., 2020). At this stage, isotopic effects of thermodynamic/equilibrium are predominant controlling factors, and isotopic exchange reactions occur under these conditions (Cesar et al., 2020). When the thermal maturity further increases, isotopic effects of thermodynamic/equilibrium are no longer the predominant controlling factors, and other processes may become more important; thus, carbon isotopic reversal first occurs in ethane and then in propane (Dai et al., 2016a; Cesar et al., 2020). In general, according to the published data, it is clear that with increasing thermal maturity, ethane and propane first become more enriched in  $^{13}\text{C}$ , then become more depleted in  $^{13}\text{C}$ , and finally become more enriched in  $^{13}\text{C}$  again (Ferworn et al., 2008; Burruss and Laughrey, 2010; Rodriguez and Philp, 2010; Zumberge et al., 2012; Hao and Zou, 2013; Tilley and Muehlenbachs, 2013; Dai et al., 2014a; Dai et al., 2016b; Dai et al., 2017; Liu et al., 2018; Ni et al., 2018; Xia and Gao, 2018; Feng et al., 2020) (Figures 7B, C). The Wufeng–Longmaxi shale gases from the Taiyang, Jiaoshiba, and Weirong shale gas fields fall in the post-rollover area, where ethane and propane are still depleted at  $^{13}\text{C}$ , but the carbon isotopic compositions get to be more positive again (Figures 7B, C).

Among the mechanisms which have been invoked to account for the carbon isotopic depletion in ethane and propane, most of them are related to high temperatures, for example, 1) *in situ* cracking of  $\text{C}_{2+}$  gas (Ferworn et al., 2008), *in situ* cracking of oil or gas (Rodriguez and Philp, 2010), simultaneous cracking of kerogen, oil, and gas in a closed system (Tilley et al., 2011), and cracking of kerogen-entrapped straight-chain aliphatic hydrocarbons (Ni et al., 2018); 2) water reacting with  $\text{CH}_4$  to form isotopically light  $\text{CO}_2$  and hydrogen and  $\text{CO}_2$  and hydrogen, subsequently forming isotopically light ethane and propane (Zumberge et al., 2012); 3) Rayleigh fractionation of ethane and propane involving redox reactions with transition metals and water at temperatures on the order of  $250^\circ\text{C}$ – $300^\circ\text{C}$  (Burruss and Laughrey, 2010); 4) Diffusive migration during the stage with high maturity (Dai et al., 2016a). As discussed above, Fischer–Tropsch-type synthesis of hydrocarbon from  $\text{CO}_2$  and  $\text{H}_2$  has contributed to the carbon isotopic depletion in ethane and propane, but due to the limited amount of the reactant, it cannot be the controlling factor. In the southern Sichuan Basin, wet gas cracking cannot explain the depletion of  $^{13}\text{C}$  in ethane and propane.  $\text{C}_{2+}$  wet gas cracking at elevated temperatures will increase  $\text{C}_2/\text{C}_3$  ratio and thus a decrease in gas wetness (Prinzhofer and Huc, 1995). The Wufeng–Longmaxi shale gas is characterized by very low gas wetness,

and the content of ethane and propane is generally less than 1. Wet gas cracking of pentanes and butanes will cause enrichment in  $^{12}\text{C}$  in ethane and propane (Xia et al., 2013); however, under the over-mature dry gas stage, cracking of ethane and propane possibly occurs and the residual ethane and propane will become more enriched in  $^{13}\text{C}$  due to the kinetic isotopic fractionation effects (Tang et al., 2000). Obviously, this is opposite to the phenomenon of the Wufeng–Longmaxi shale gas.

Actually, Xia and Gao (2018) stated that mechanisms such as mixing of primary and secondary products in source rocks (Rodriguez and Philp, 2010; Ni et al., 2018; Hao and Zou, 2013; Ferworn et al., 2008; Xia et al., 2013) and water-involved reactions (Burruss and Laughrey, 2010; Gao et al., 2014; Zhang et al., 2018b; Zumberge et al., 2012) cannot satisfy the isotopic and mass balance requirements and proposed that the depletion of  $^{13}\text{C}$  in ethane and propane resulted from the reversible conversion from alkane to alkyl groups. The isotope effect is dependent on the rate and kinetic isotope effects of these reversible free-radical reactions catalyzed by minerals, and the isotopic depletion in  $^{13}\text{C}$  is consistent with the extent of the decomposition (Xia and Gao, 2018). However, these free-radical reactions may proceed in very different ways in different locations since the free-radical concentrations may vary greatly in different geological environments. In the sandstone and limestone formations, there is no sufficient hydrogen donors, and the reversal reactions will be suppressed and the fractionation will proceed likely in a Rayleigh fractionation mode; while organic-rich shales have abundant hydrogen donor, so the reversible reaction is possible, and the isotopic reversal is commonly found in either conventional and unconventional natural gases at relatively high thermal mature stages (Xia and Gao, 2018). The Upper Ordovician Wufeng–Lower Silurian Longmaxi shale comprises black shale, siliceous shale, calcareous-siliceous shale, and argillaceous-siliceous shale (Zou et al., 2019). It is deposited in a deep water environment and dominated by Type I and II<sub>1</sub> organic matter and typically has TOC of around 3% in the Taiyang, Jiaoshiba, and Weirong areas (Dai et al., 2014a; Liang et al., 2020a; Liang et al., 2020b; Zou et al., 2021). During the Hirnantian Stage glacial interval (Middle and Upper Wufeng Formation), there was a rapid global fall in sea level, while the  $\text{P}_2\text{O}_5/\text{TiO}_2$  ratio reached 0.84 and the southern Sichuan Basin still experienced plankton bloom, high paleo-productivity, and high burial rates of organic matter (Zou et al., 2019). During the Rhuddanian Stage (Lower Longmaxi Formation), sea level increased and plankton bloomed, resulting in the widespread deposition of back shale in deep, oxygen-poor conditions under high-productivity surface waters (Zou et al., 2019). In southern China, Silurian marine source rocks with restored hydrogen index greater than 600 mg/g TOC account for 43%, and samples with restored hydrogen index between 250–600 mg/g TOC account for 57% (Zhang et al., 2013). In addition, the Wufeng–Longmaxi shale reached over  $180^\circ\text{C}$  in Late Permian in the Taiyang area and reached over  $200^\circ\text{C}$  in Late Jurassic in the Jiaoshiba area (He et al., 2017; Liang et al., 2020b; Pang et al., 2019; Tenger et al., 2017; Xiong et al., 2021). In general, the Wufeng–Longmaxi shale has equivalent vitrinite reflectance Ro% of 2.73%–4.62% (Wang et al., 2019; Zou et al., 2021) and gas wetness between 0.09% and 0.97%. Therefore, the Wufeng–Longmaxi shale is abundant in hydrogen donors and at a high thermal maturation stage with a high conversion rate. When



plotting the Wufeng–Longmaxi shale gases into the  $\delta^{13}\text{C}_2$  value versus gas wetness plot of the Barnett shale gases by Xia and Gao (2018), the carbon isotopic fractionation of ethane of the Wufeng–Longmaxi shale gases agrees well with the calculated results (pink line in Figure 12), which mainly fall in the post-rollover stage and indicates high thermal maturity of the gas. As indicated by the reversible free-radical reactions, the isotopic compositions are positive at the stage of low conversion ratios and then become negative with increasing conversion ratios; When the conversion ratios get even higher and the remaining reactant becomes even less, the isotopic compositions become more positive again (Xia and Gao, 2018). As for the Wufeng–Longmaxi shale gas, the extremely low content of ethane and propane ( $\text{C}_{2+3} < 1\%$ ) indicates high conversion ratios, so during the late catagenesis stage, decomposition of ethane and propane is accompanied by the depletion of  $^{13}\text{C}$  in the residual ethane and propane, but in general, the isotopic composition becomes more positive again and falls in the post-rollover area. During this over-mature stage, reactions of free-radical decomposition are important controlling factors, resulting in the depletion of  $^{13}\text{C}$  in ethane and propane, which prevail the thermal cracking reactions.

## 6 CONCLUSION

Molecular and stable carbon isotopic compositions of gases from the Wufeng–Longmaxi shale in the Taiyang (shallow), Jiaoshiba (middle), and Weirong (deep) shale gas fields in the Sichuan Basin have been investigated. All the gases are dominated by

methane and have very low gas wetness (generally  $< 0.83$ ). Methane accounts for 98.82%, 98.13%, and 96.91% in the Taiyang, Jiaoshiba, and Weirong shale gas fields, respectively. The average carbon isotopic value of methane is  $-35.2\text{‰}$  in Weirong,  $-30.3\text{‰}$  in Jiaoshiba, and  $-28.5\text{‰}$  in Taiyang shale gas fields. The enrichment of  $^{13}\text{C}$  in methane is mainly caused by the extremely high thermal maturity. Shale gases from the Jiaoshiba and Taiyang gas fields fall offset from the  $\delta^{13}\text{C}_1$ –wetness linear trend line by the Weirong, Barnett, and Fayetteville shale gases, which is due to the contribution from the Fischer–Tropsch-type synthesis of hydrocarbon gas from  $\text{CO}_2$  and  $\text{H}_2$ . When thermal cracking gas is mixed with the hydrocarbon gas generated by the Fischer–Tropsch-type synthesis, it will significantly increase the amount of wet gas, but has little impact on methane. In the Taiyang shale gas field, when burial depth changes from  $\sim 2300$  to  $\sim 900$  m,  $\delta^{13}\text{C}_1$ ,  $\delta^{13}\text{C}_2$ , and  $\delta^{13}\text{C}_3$  values decrease by  $\sim 3\text{‰}$ , and a linear correlation exists between carbon isotope and burial depth. This is mainly caused by diffusive migration. Shale gases from the Taiyang, Jiaoshiba, and Weirong gas fields are characterized by a complete carbon isotopic reversal trend among the  $\text{C}_1$ – $\text{C}_3$  alkane gases ( $\delta^{13}\text{C}_1 > \delta^{13}\text{C}_2 > \delta^{13}\text{C}_3$ ). This is mainly caused by the reversible free-radical reactions with the conversion from alkane to alkyl groups with a minor contribution from the Fischer–Tropsch-type synthesis.

## DATA AVAILABILITY STATEMENT

The original contributions presented in the study are included in the article/Supplementary Material; further inquiries can be directed to the corresponding authors.

## AUTHOR CONTRIBUTIONS

YN: manuscript design and writing. DD: manuscript writing of geological information. LY and JC: data collection and manuscript revision. XL and FL: sample collection. JL: sample collection. JHG: sample analyses. JLG: data collection.

## FUNDING

This study is funded by the National Key Research and Development Projects of China (Grant No. 2019YFC1805505) and the PetroChina Scientific Research and Technology Development Project (Grant Nos. 2021DJ05, 2017D-5008-08).

## ACKNOWLEDGMENTS

We thank Prof. Jinxing Dai and Dr. Yuman Wang from the PetroChina Research Institute of Petroleum Exploration and Development for helpful and open discussion. We thank the reviewers for their thorough reviews and constructive suggestions, which improve the manuscript greatly.

## REFERENCES

- Bergström, S. M., Saltzman, M. M., and Schmitz, B. (2006). First Record of the Hirnantian (Upper Ordovician)  $\delta^{13}\text{C}$  Excursion in the North American Midcontinent and its Regional Implications. *Geol. Mag.* 143, 657–678.
- Bernard, B. B., Brooks, J. M., and Sackett, W. M. (1976). Natural Gas Seepage in the Gulf of Mexico. *Earth Planet. Sci. Lett.* 31, 48–54. doi:10.1016/0012-821x(76)90095-9
- Berner, U., and Faber, E. (1996). Empirical Carbon Isotope/maturity Relationships for Gases from Algal Kerogens and Terrigenous Organic Matter, Based on Dry, Open-System Pyrolysis. *Org. Geochem.* 24, 947–955. doi:10.1016/s0146-6380(96)00090-3
- Brenchley, P. J., Marshall, J. D., Carden, G. A. F., Robertson, D. B. R., Long, D. G. F., Meidla, T., et al. (1994). Bathymetric and Isotopic Evidence for a Short-Lived Late Ordovician Glaciation in a Greenhouse Period. *Geology* 22, 295–298. doi:10.1130/0091-7613(1994)022<0295:baiefa>2.3.co;2
- Burruss, R. C., and Laughrey, C. D. (2010). Carbon and Hydrogen Isotopic Reversals in Deep Basin Gas: Evidence for Limits to the Stability of Hydrocarbons. *Org. Geochem.* 41, 1285–1296. doi:10.1016/j.orggeochem.2010.09.008
- Cao, C., Zhang, M., Li, L., Wang, Y., Li, Z., Du, L., et al. (2020). Tracing the Sources and Evolution Processes of Shale Gas by Coupling Stable (C, H) and Noble Gas Isotopic Compositions: Cases from Weiyuan and Changning in Sichuan Basin, China. *J. Nat. Gas Sci. Eng.* 78, 103304. doi:10.1016/j.jngse.2020.103304
- Cesar, J., Nightingale, M., Becker, V., and Mayer, B. (2020). Stable Carbon Isotope Systematics of Methane, Ethane and Propane from Low-Permeability Hydrocarbon Reservoirs. *Chem. Geol.* 558, 119907. doi:10.1016/j.chemgeo.2020.119907
- Chen, C. (2018). *Research on Paleogeography, Paleoclimate and Formation Mechanism of Source Rock during Geologic Transition Period from Late Ordovician to Early Silurian in Southern Sichuan Province - Northern Guizhou Province, South China*. Wuhan: China University of Geosciences (Wuhan). Ph.D thesis.
- Chen, J., Li, W., Ni, Y., Dai, X., Liang, D., Deng, C., et al. (2018). The Permian Source Rocks in the Sichuan Basin and its Natural Gas Exploration Potential (Part 2): Geochemical Characteristics of Source Rocks and Latent Capacity of Natural Gas Resources. *Nat. Gas. Ind.* 38, 33–45.
- Chen, J., Li, C., Shen, P., and Ying, G. (1995). Carbon and Hydrogen Isotopic Characteristics of Hydrocarbons in Coal Type Gas from China. *Sedimentol. Sin.* 13, 59–69.
- Chen, Z., Chen, L., Wang, G., Zou, C., Jiang, S., Si, Z., et al. (2020). Applying Isotopic Geochemical Proxy for Gas Content Prediction of Longmaxi Shale in the Sichuan Basin, China. *Mar. Petroleum Geol.* 116, 104329. doi:10.1016/j.marpetgeo.2020.104329
- Chung, H. M., Gormly, J. R., and Squires, R. M. (1988). Origin of Gaseous Hydrocarbons in Subsurface Environments: Theoretical Considerations of Carbon Isotope Distribution. *Chem. Geol.* 71, 97–104. doi:10.1016/0009-2541(88)90108-8
- Clayton, C. (1991). Carbon Isotope Fractionation during Natural Gas Generation from Kerogen. *Mar. Petroleum Geol.* 8, 232–240. doi:10.1016/0264-8172(91)90010-x
- Curiale, J. A., and Curtis, J. B. (2016). Organic Geochemical Applications to the Exploration for Source-Rock Reservoirs - A Review. *J. Unconv. Oil Gas Resour.* 13, 1–31. doi:10.1016/j.juogr.2015.10.001
- Dai, J., Gong, D., Ni, Y., Huang, S., and Wu, W. (2014b). Stable Carbon Isotopes of Coal-Derived Gases Sourced from the Mesozoic Coal Measures in China. *Org. Geochem.* 74, 123–142. doi:10.1016/j.orggeochem.2014.04.002
- Dai, J. (1992). Identification and Distinction of Various Alkane Gases. *Sci. China (Chem.)* 35, 1246–1257.
- Dai, J., Liao, F., and Ni, Y. (2013). Discussions on the gas source of the Triassic Xujiahe Formation tight sandstone gas reservoirs in Yuanba and Tongnanba, Sichuan Basin: An answer to Yinfeng et al. *Pet. Explor. Dev.* 40, 250–256. doi:10.1016/s1876-3804(13)60033-6
- Dai, J., Ni, Y., Gong, D., Feng, Z., Liu, D., Peng, W., et al. (2017). Geochemical Characteristics of Gases from the Largest Tight Sand Gas Field (Sulige) and Shale Gas Field (Fuling) in China. *Mar. Petroleum Geol.* 79, 426–438. doi:10.1016/j.marpetgeo.2016.10.021
- Dai, J., Ni, Y., Huang, S., Gong, D., Liu, D., Feng, Z., et al. (2016a). Secondary Origin of Negative Carbon Isotopic Series in Natural Gas. *J. Nat. Gas Geoscience* 1, 1–7. doi:10.1016/j.jnggs.2016.02.002
- Dai, J., Ni, Y., Liu, Q., Wu, X., Yu, C., Gong, D., et al. (2022). Carbon Dioxide and its Carbon Isotopic Composition of Natural Gas in the Sichuan Basin, SW China. *Front. Earth Sci.* 10, 857876. doi:10.3389/feart.2022.857876
- Dai, J., Ni, Y., and Zou, C. (2012a). Stable Carbon and Hydrogen Isotopes of Natural Gases Sourced from the Xujiahe Formation in the Sichuan Basin, China. *Org. Geochem.* 43, 103–111. doi:10.1016/j.orggeochem.2011.10.006
- Dai, J., Ni, Y., Zou, C., Tao, S., Hu, G., Hu, A., et al. (2009). Stable Carbon Isotopes of Alkane Gases from the Xujiahe Coal Measures and Implication for Gas-Source Correlation in the Sichuan Basin, SW China. *Org. Geochem.* 40, 638–646. doi:10.1016/j.orggeochem.2009.01.012
- Dai, J., Pei, X., and Qi, H. (1992). *Natural Gas Geology in China (Volume I)*. Beijing: Petroleum Industry Press.
- Dai, J. (2003). Pool-forming Periods and Gas Sources of Weiyuan Gasfield. *Pet. Geol. exper.* 25 (5), 473–780.
- Dai, J., and Qi, H. (1989). Relationship of  $\delta^{13}\text{C}$ -Ro of Coal-Derived Gas in China. *Chin. Sci. Bull.* 34, 690–692.
- Dai, J. X., Ni, Y., Liu, Q., Wu, X., Gong, D., Hong, F., et al. (2021). Sichuan Super Gas Basin. *Pet. Explor. Dev.* 48, 1–8. doi:10.1016/s1876-3804(21)60284-7
- Dai, J., Xia, X., Li, Z., Coleman, D. D., Dias, R. F., Gao, L., et al. (2012b). Inter-laboratory Calibration of Natural Gas Round Robins for  $\delta^2\text{H}$  and  $\delta^{13}\text{C}$  Using Off-Line and On-Line Techniques. *Chem. Geol.* 310–311, 49–55. doi:10.1016/j.chemgeo.2012.03.008
- Dai, J., Zou, C., Dong, D., Ni, Y., Wu, W., Gong, D., et al. (2016b). Geochemical Characteristics of Marine and Terrestrial Shale Gas in China. *Mar. Petroleum Geol.* 76, 444–463. doi:10.1016/j.marpetgeo.2016.04.027
- Dai, J., Zou, C., Liao, S., Dong, D., Ni, Y., Huang, J., et al. (2014a). Geochemistry of the Extremely High Thermal Maturity Longmaxi Shale Gas, Southern Sichuan Basin. *Org. Geochem.* 74, 3–12. doi:10.1016/j.orggeochem.2014.01.018
- Fan, J., Peng, P. a., and Melchin, M. J. (2009). Carbon Isotopes and Event Stratigraphy Near the Ordovician-Silurian Boundary, Yichang, South China. *Palaeogeogr. Palaeoclimatol. Palaeoecol.* 276, 160–169. doi:10.1016/j.palaeo.2009.03.007
- Feng, Z., Dong, D., Tian, J., Qiu, Z., Wu, W., and Zhang, C. (2018). Geochemical Characteristics of Longmaxi Formation Shale Gas in the Weiyuan Area, Sichuan Basin, China. *J. Petroleum Sci. Eng.* 167, 538–548. doi:10.1016/j.petrol.2018.04.030
- Feng, Z., Dong, D., Tian, J., Wu, W., Cai, Y., Shi, Z., et al. (2019). Geochemical Characteristics of Lower Silurian Shale Gas in the Changning-Zhaotong Exploration Blocks, Southern Periphery of the Sichuan Basin. *J. Petroleum Sci. Eng.* 174, 281–290. doi:10.1016/j.petrol.2018.11.022
- Feng, Z., Hao, F., Dong, D., Zhou, S., Wu, W., Xie, C., et al. (2020). Geochemical Anomalies in the Lower Silurian Shale Gas from the Sichuan Basin, China: Insights from a Rayleigh-type Fractionation Model. *Org. Geochem.* 142, 103981. doi:10.1016/j.orggeochem.2020.103981
- Feng, Z., Liu, D., Huang, S., Wu, W., Dong, D., Peng, W., et al. (2016). Carbon Isotopic Composition of Shale Gas in the Silurian Longmaxi Formation of the Changning Area, Sichuan Basin. *Petroleum Explor. Dev.* 43, 769–777. doi:10.1016/s1876-3804(16)30092-1
- Ferworn, K., Zumberge, J., Reed, J., and Brown, S. (2008). *Gas Character Anomalies Found in Highly Productive Shale Gas Wells*. Houston, TX. [http://www.zenzebra.net/quebec/Ferworn\\_et\\_al\\_2008.pdf](http://www.zenzebra.net/quebec/Ferworn_et_al_2008.pdf).
- Gao, J., Liu, J., and Ni, Y. (2018). Gas Generation and its Isotope Composition during Coal Pyrolysis: The Catalytic Effect of Nickel and Magnetite. *Fuel* 222, 74–82. doi:10.1016/j.fuel.2018.02.118
- Gao, L., Schimmelmann, A., Tang, Y., and Mastalerz, M. (2014). Isotope Rollover in Shale Gas Observed in Laboratory Pyrolysis Experiments: Insight to the Role of Water in Thermogenesis of Mature Gas. *Org. Geochem.* 68, 95–106. doi:10.1016/j.orggeochem.2014.01.010
- Hao, F., and Zou, H. (2013). Cause of Shale Gas Geochemical Anomalies and Mechanisms for Gas Enrichment and Depletion in High-Maturity Shales. *Mar. Petroleum Geol.* 44, 1–12. doi:10.1016/j.marpetgeo.2013.03.005
- He, Z. L., Hu, Z. Q., Nie, H. K., Li, S. J., and Xu, J. (2017). Characterization of Shale Gas Enrichment in the Wufeng-Longmaxi Formation in the Sichuan Basin and its Evaluation of Geological Construction-Transformation Evolution Sequence. *Nat. Gas. Geosci.* 28, 724–733.

- Huang, S. P., Jiang, Q. C., Wang, Z. C., Su, W., Feng, Q. F., and Feng, Z. Q. (2016). Differences between the Middle Permian Qixia and Maokou Source Rocks in the Sichuan Basin. *Nat. Gas. Ind.* 36, 26–34.
- Jacobson, S. R., Hatch, J. R., Teerman, S. C., and Askin, R. A. (1988). Middle Ordovician Organic Matter Assemblages and Their Effect on Ordovician-Derived Oils. *AAPG Bull.* 72, 1090–1100. doi:10.1306/703c97c6-1707-11d7-8645000102c1865d
- James, A. T. (1983). Correlation of Natural Gas by Use of Carbon Isotopic Distribution between Hydrocarbon Components. *Am. Assoc. Pet. Geol. Bull.* 67, 1176–1191. doi:10.1306/03b5b722-16d1-11d7-8645000102c1865d
- Kump, L. R., Arthur, M. A., Patzkowsky, M. E., Gibbs, M. T., Pinkus, D. S., and Sheehan, P. M. (1999). A Weathering Hypothesis for Glaciation at High Atmospheric pCO<sub>2</sub> during the Late Ordovician. *Palaeogeogr. Palaeoclimatol. Palaeoecol.* 152, 173–187. doi:10.1016/s0031-0182(99)00046-2
- Li, W., Lu, S., Li, J., Zhang, P., Wang, S., Feng, W., et al. (2020). Carbon Isotope Fractionation during Shale Gas Transport: Mechanism, Characterization and Significance. *Sci. China Earth Sci.* 63, 674–689. doi:10.1007/s11430-019-9553-5
- Liang, D., Zhang, S., Zhao, M., and Wang, F. (2002). Hydrocarbon Sources and Stages of Reservoir Formation in Kuqa depression, Tarim Basin. *Chin. Sci. Bull.* 47, 56–63. doi:10.1007/bf02902820
- Liang, M., Tan, X., Chen, X., Wang, J., Ran, T., Wang, P., et al. (2018). Sequence Stratigraphy of Wufeng-Longmaxi Formation in the Southeastern Chongqing Area and its Geological Significance. *Coal Geol. Explor.* 46, 40–51.
- Liang, X., Xu, Z., Zhang, Z., Wang, W., Zhang, J., Lu, H., et al. (2020b). Breakthrough of Shallow Shale Gas Exploration in Taiyang Anticline Area and its Significance for Resource Development in Zhaotong, Yunnan Province, China. *Pet. Explor. Dev.* 47, 11–28. doi:10.1016/s1876-3804(20)60002-7
- Liang, X., Xu, Z., Zhang, J., Zhang, Z., Li, Z., Jiang, P., et al. (2020a). Key Efficient Exploration and Development Technologies of Shallow Shale Gas: a Case Study of Taiyang Anticline Area of Zhaotong National Shale Gas Demonstration Zone. *Acta Pet. Sin.* 41, 1033–1048.
- Liang, X., Shan, C., Zhang, Z., Xu, J., Wang, W., Zhang, J., et al. (2021). Three-dimensional Closed System" Accumulation Model of Taiyang Anticline Mountain Shallow Shale Gas in Zhaotong Demonstration Area. *Acta Geol. Sin.* 95, 1–20.
- Lin, J., Hu, H., and Liang, Q. (2017). Geochemical Characteristics and Implications of Shale Gas in Jiaoshiba, Eastern China. *Earth Sci.* 42, 1124–1133.
- Liu, Q., Jin, Z., Wang, X., Yi, J., Meng, Q., Wu, X., et al. (2018). Distinguishing Kerogen and Oil Cracked Shale Gas Using H, C-Isotopic Fractionation of Alkane Gases. *Mar. Petroleum Geol.* 91, 350–362. doi:10.1016/j.marpetgeo.2018.01.006
- Lorant, F., Prinzhofer, A., Behar, F., and Huc, A.-Y. (1998). Carbon Isotopic and Molecular Constraints on the Formation and the Expulsion of Thermogenic Hydrocarbon Gases. *Chem. Geol.* 147, 249–264. doi:10.1016/s0009-2541(98)00017-5
- Ma, Y., Zhong, N., Yao, L., Huang, H., Larter, S., and Jiao, W. (2020). Shale Gas Desorption Behavior and Carbon Isotopic Variations of Gases from Canister Desorption of Two Sets of Gas Shales in South China. *Mar. Petroleum Geol.* 113, 104127. doi:10.1016/j.marpetgeo.2019.104127
- Marshall, J. D., Brenchley, P. J., Mason, P., Wolff, G. A., Astini, R. A., Hints, L., et al. (1997). Global Carbon Isotopic Events Associated with Mass Extinction and Glaciation in the Late Ordovician. *Palaeogeogr. Palaeoclimatol. Palaeoecol.* 132, 195–210. doi:10.1016/s0031-0182(97)00063-1
- Martini, A. M., Walter, L. M., and McIntosh, J. C. (2008). Identification of Microbial and Thermogenic Gas Components from Upper Devonian Black Shale Cores, Illinois and Michigan Basins. *Bulletin* 92, 327–339. doi:10.1306/10180706037
- Mi, J., He, K., Shuai, Y., and Guo, J. (2022). *Combination of Methyl from Methane Early Cracking: A Possible Mechanism for Carbon Isotopic Reversal of Overmature Natural Gas*. Geofluids, 9965046.
- Milkov, A. V. (2021). New Approaches to Distinguish Shale-Sourced and Coal-Sourced Gases in Petroleum Systems. *Org. Geochem.* 158, 104271. doi:10.1016/j.orggeochem.2021.104271
- Ni, Y., Gao, J., Chen, J., Liao, F., Liu, J., and Zhang, D. (2018). Gas Generation and its Isotope Composition during Coal Pyrolysis: Potential Mechanism of Isotope Rollover. *Fuel* 231, 387–395. doi:10.1016/j.fuel.2018.05.029
- Ni, Y., Liao, F., Dai, J., Zou, C., Wu, X., Zhang, D., et al. (2014). Studies on Gas Origin and Gas Source Correlation Using Stable Carbon Isotopes - A Case Study of the Giant Gas Fields in the Sichuan Basin, China. *Energy Explor. Exploitation* 32, 41–74. doi:10.1260/0144-5987.32.1.41
- Ni, Y., Liao, F., Gao, J., Chen, J., Yao, L., and Zhang, D. (2019a). Hydrogen Isotopes of Hydrocarbon Gases from Different Organic Facies of the Zhongba Gas Field, Sichuan Basin, China. *J. Petroleum Sci. Eng.* 179, 776–786. doi:10.1016/j.petrol.2019.04.102
- Ni, Y., Liao, F., Yao, L., Gao, J., and Zhang, D. (2019b). Hydrogen Isotope of Natural Gas from the Xujiahe Formation and its Implications for Water Salinization in Central Sichuan Basin, China. *J. Nat. Gas Geoscience* 4, 215–230. doi:10.1016/j.jnggs.2019.08.003
- Ni, Y., Ma, Q., Ellis, G. S., Dai, J., Katz, B., Zhang, S., et al. (2011). Fundamental Studies on Kinetic Isotope Effect (KIE) of Hydrogen Isotope Fractionation in Natural Gas Systems. *Geochimica Cosmochimica Acta* 75, 2696–2707. doi:10.1016/j.gca.2011.02.016
- Ni, Y., Zhang, D., Liao, F., Gong, D., Xue, P., Yu, F., et al. (2015). Stable Hydrogen and Carbon Isotopic Ratios of Coal-Derived Gases from the Turpan-Hami Basin, NW China. *Int. J. Coal Geol.* 152, 144–155. doi:10.1016/j.coal.2015.07.003
- Orth, C. J., Gilmore, J. S., Quintana, L. R., and Sheehan, P. M. (1986). Terminal Ordovician Extinction: Geochemical Analysis of the Ordovician/Silurian Boundary, Anticosti Island, Quebec. *Geol.* 14, 433–436. doi:10.1130/0091-7613(1986)14<433:toegao>2.0.co;2
- Pancost, R. D., Freeman, K. H., Herrmann, A. D., Patzkowsky, M. E., Ainsaar, L., and Martma, T. (2013). Reconstructing Late Ordovician Carbon Cycle Variations. *Geochimica Cosmochimica Acta* 105, 433–454. doi:10.1016/j.gca.2012.11.033
- Pancost, R. D., Freeman, K. H., and Patzkowsky, M. E. (1999). Organic-matter Source Variation and the Expression of a Late Middle Ordovician Carbon Isotope Excursion. *Geol.* 27, 1015–1018. doi:10.1130/0091-7613(1999)027<1015:omsvat>2.3.co;2
- Pang, H. Q., Xiong, L., Wei, L., Shi, H., Dong, X., Zhang, T., et al. (2019). Analysis of Main Geological Factors for Enrichment and High Yield of Deep Shale Gas in Southern Sichuan: A Case Study of Weirong Shale Gas Field. *Nat. Gas. Ind.* 39, 78–84.
- Pernaton, E., Prinzhofer, A., and Schneider, F. (1996). Reconsideration of Methane Isotope Signature as a Criterion for the Genesis of Natural Gas: Influence of Migration on Isotopic Signatures. *Rev. Inst. Fr. Pét.* 51, 635–651. doi:10.2516/ogst:1996042
- Prinzhofer, A. A., and Huc, A. Y. (1995). Genetic and Post-genetic Molecular and Isotopic Fractionations in Natural Gases. *Chem. Geol.* 126, 281–290. doi:10.1016/0009-2541(95)00123-9
- Prinzhofer, A., and Pernaton, É. (1997). Isotopically Light Methane in Natural Gas: Bacterial Imprint or Diffusive Fractionation? *Chem. Geol.* 142, 193–200. doi:10.1016/s0009-2541(97)00082-x
- Qing, H., and Veizer, J. (1994). Oxygen and Carbon Isotopic Composition of Ordovician Brachiopods: Implications for Coeval Seawater. *Geochimica Cosmochimica Acta* 58, 4429–4442. doi:10.1016/0016-7037(94)90345-x
- Rodriguez, N. D., and Philp, R. P. (2010). Geochemical Characterization of Gases from the Mississippian Barnett Shale, Fort Worth Basin, Texas. *Bulletin* 94, 1641–1656. doi:10.1306/04061009119
- Rong, J., Chen, X., Wang, Y., Zhan, R., Liu, J., Huang, B., et al. (2011). Northward Expansion of Central Guizhou Oldland through the Ordovician and Silurian Transition: Evidence and Implication. *Sci. China* 41, 1407–1415.
- Rong, J., Wang, Y., Zhan, R., Fan, J., Huang, B., Tang, P., et al. (2019). Silurian Integrative Stratigraphy and Timescale of China. *Sci. China Earth Sci.* 49, 93–114. doi:10.1007/s11430-017-9258-0
- Schoell, M. (1980). The Hydrogen and Carbon Isotopic Composition of Methane from Natural Gases of Various Origins. *Geochimica Cosmochimica Acta* 44, 649–661. doi:10.1016/0016-7037(80)90155-6
- Stahl, W. J., and Carey, B. D. (1975). Source-rock Identification by Isotope Analyses of Natural Gases from Fields in the Val Verde and Delaware Basins, West Texas. *Chem. Geol.* 16, 257–267. doi:10.1016/0009-2541(75)90065-0
- Strapoc, D., Mastalerz, M., Schimmelmann, A., Drobniak, A., and Hasenmueller, N. R. (2010). Geochemical Constraints on the Origin and Volume of Gas in the New Albany Shale (Devonian–Mississippian), Eastern Illinois Basin. *AAPG Bull.* 94, 1713–1740.
- Tang, Y. C., and Xia, X. Y., (2011). *Quantitative Assessment of Shale Gas Potential Based on its Special Generation and Accumulation Processes*. Abstract, Search and Discovery Article #40819., American Association of Petroleum Geologist

- Annual Meeting, Houston, p. <[http://www.searchanddiscovery.com/documents/2011/40819tang/ndx\\_tang.pdf](http://www.searchanddiscovery.com/documents/2011/40819tang/ndx_tang.pdf).
- Tang, Y., Perry, J. K., Jenden, P. D., and Schoell, M. (2000). Mathematical Modeling of Stable Carbon Isotope Ratios in Natural Gases. *Geochimica Cosmochimica Acta* 64, 2673–2687. doi:10.1016/s0016-7037(00)00377-x
- Tenger, B., Shen, B., Yu, L., Yang, Y., Zhang, W., Tao, C., et al. (2017). Mechanism of Shale Gas Generation and Accumulation in the Ordovician Wufeng-Longmaxi Formation, Sichuan Basin, SW China. *Pet. explor. Dev.* 44, 69–78.
- Tilley, B., McLellan, S., Hiebert, S., Quartero, B., Veilleux, B., and Muehlenbachs, K. (2011). Gas Isotope Reversals in Fractured Gas Reservoirs of the Western Canadian Foothills: Mature Shale Gases in Disguise. *Bulletin* 95, 1399–1422. doi:10.1306/01031110103
- Tilley, B., and Muehlenbachs, K. (2013). Isotope Reversals and Universal Stages and Trends of Gas Maturation in Sealed, Self-Contained Petroleum Systems. *Chem. Geol.* 339, 194–204. doi:10.1016/j.chemgeo.2012.08.002
- Wang, G., Ma, Y., Zhao, Y., and Chen, W. (2021). Carbon Isotope Fractionation during Shale Gas Transport through Organic and Inorganic Nanopores from Molecular Simulations. *Energy Fuels* 35, 11992–12004. doi:10.1021/acs.energyfuels.1c01448
- Wang, K., Chatterton, B. D. E., and Wang, Y. (1997). An Organic Carbon Isotope Record of Late Ordovician to Early Silurian Marine Sedimentary Rocks, Yangtze Sea, South China: Implications for CO<sub>2</sub> Changes during the Hirnantian Glaciation. *Palaeogeogr. Palaeoclimatol. Palaeoecol.* 132, 147–158. doi:10.1016/s0031-0182(97)00046-1
- Wang, K., Orth, C. J., Attrep, M., Chatterton, B. D. E., Wang, X., and Li, J.-j. (1993). The Great Latest Ordovician Extinction on the South China Plate: Chemostratigraphic Studies of the Ordovician-Silurian Boundary Interval on the Yangtze Platform. *Palaeogeogr. Palaeoclimatol. Palaeoecol.* 104, 61–79. doi:10.1016/0031-0182(93)90120-8
- Wang, Y., Qiu, N., Yang, Y., Rui, X., Zhou, Y., Fang, G., et al. (2019). Thermal Maturity of Wufeng-Longmaxi Shale in Sichuan Basin. *Earth Sci.* 44, 953–971.
- Wei, X., Guo, T., and Liu, R. (2016). Geochemical Features of Shale Gas and Their Genesis in Jiaoshiha Block of Fuling Shale Gasfield, Chongqing. *Nat. Gas. Geosci.* 27, 539–548.
- Wu, W., Fang, C., Dong, D., and Liu, D. (2015). Shale Gas Geochemical Anomalies and Gas Source Identification. *Acta Pet. Sin.* 36, 1332–1340+1366.
- Wu, W., Huang, S., Hu, G., and Gong, D. (2014). A Comparison between Shale Gas and Conventional Gas on Geochemical Characteristics in Weiyuan Area. *Nat. Gas. Geosci.* 25, 1994–2002.
- Xia, X., Chen, J., Braun, R., and Tang, Y. (2013). Isotopic Reversals with Respect to Maturity Trends Due to Mixing of Primary and Secondary Products in Source Rocks. *Chem. Geol.* 339, 205–212. doi:10.1016/j.chemgeo.2012.07.025
- Xia, X., and Gao, Y. (2018). Depletion of <sup>13</sup>C in Residual Ethane and Propane during Thermal Decomposition in Sedimentary Basins. *Org. Geochem.* 125, 121–128. doi:10.1016/j.orggeochem.2018.09.003
- Xia, X., and Tang, Y. (2012). Isotope Fractionation of Methane during Natural Gas Flow with Coupled Diffusion and Adsorption/desorption. *Geochimica Cosmochimica Acta* 77, 489–503. doi:10.1016/j.gca.2011.10.014
- Xiong, L., Pang, H. Q., Zhao, Y., Wei, L. M., Zhou, H., and Cao, Q. (2021). Micro Pore Structure Characterization and Classification Evaluation of Reservoirs in Weirong Deep Shale Gas Field. *Reserv. Eval. Dev.* 11, 20–29.
- Xu, S. L., Chen, H. D., Chen, A. Q., Lin, L. B., Li, J. W., and Yang, J. B. (2011). Source Rock Characteristics of Marine Strata, Sichuan Basin. *J. Jilin Univ. (Earth Sci. Ed.)* 41, 343–350.
- Yan, D., Chen, D., Wang, Q., Wang, J., and Wang, Z. (2009). Carbon and Sulfur Isotope Anomalies across the Ordovician-Silurian Boundary on the Yangtze Platform, South China. *Palaeogeogr. Palaeoclimatol. Palaeoecol.* 274, 32–39. doi:10.1016/j.palaeo.2008.12.016
- Zhang, M., Tang, Q., Cao, C., Lv, Z., Zhang, T., Zhang, D., et al. (2018a). Molecular and Carbon Isotopic Variation in 3.5 Years Shale Gas Production from Longmaxi Formation in Sichuan Basin, China. *Mar. Petroleum Geol.* 89, 27–37. doi:10.1016/j.marpetgeo.2017.01.023
- Zhang, Q., Wang, H. Y., Bai, W. H., Lin, W., and Du, D. (2013). Restoration of Organic Matter Type in Silurian Marine Shale, South China. *Fault-Block Oil Gas Field* 20, 154–156.
- Zhang, S., He, K., Hu, G., Mi, J., Ma, Q., Liu, K., et al. (2018b). Unique Chemical and Isotopic Characteristics and Origins of Natural Gases in the Paleozoic Marine Formations in the Sichuan Basin, SW China: Isotope Fractionation of Deep and High Mature Carbonate Reservoir Gases. *Mar. Petroleum Geol.* 89, 68–82. doi:10.1016/j.marpetgeo.2017.02.010
- Zhang, T., and Krooss, B. M. (2001). Experimental Investigation on the Carbon Isotope Fractionation of Methane during Gas Migration by Diffusion through Sedimentary Rocks at Elevated Temperature and Pressure. *Geochimica Cosmochimica Acta* 65, 2723–2742. doi:10.1016/s0016-7037(01)00601-9
- Zhao, S., Kang, S., Zheng, M., Lu, S., Yang, Y., Zhang, H., et al. (2021). Prediction of Decline in Shale Gas Well Production Using Stable Carbon Isotope Technique. *Front. Earth Sci.* 15, 849–859. doi:10.1007/s11707-021-0935-4
- Zou, C. N., Zhao, Q., Cong, L., Wang, H., Shi, Z., Wu, J., et al. (2021). Development Progress, Potential and Prospect of Shale Gas in China. *Nat. Gas. Ind.* 41, 1–14.
- Zou, C. N., Dong, D., Wang, Y., Li, X., Huang, J., Wang, S., et al. (2016). Shale Gas in China: Characteristics, Challenges and Prospects (II). *Pet. explor. Dev.* 43, 166–178. doi:10.1016/s1876-3804(16)30022-2
- Zou, C., Zhu, R., Chen, Z.-Q., Ogg, J. G., Wu, S., Dong, D., et al. (2019). Organic-matter-rich Shales of China. *Earth-Science Rev.* 189, 51–78. doi:10.1016/j.earscirev.2018.12.002
- Zumbege, J., Ferworn, K., and Brown, S. (2012). Isotopic Reversal (‘rollover’) in Shale Gases Produced from the Mississippian Barnett and Fayetteville Formations. *Mar. Petroleum Geol.* 31, 43–52. doi:10.1016/j.marpetgeo.2011.06.009

**Conflict of Interest:** Authors XL and FL are employed by PetroChina Zhejiang Oilfield Company.

The remaining authors declare that the research was conducted in the absence of any commercial or financial relationships that could be construed as a potential conflict of interest.

**Publisher’s Note:** All claims expressed in this article are solely those of the authors and do not necessarily represent those of their affiliated organizations, or those of the publisher, the editors, and the reviewers. Any product that may be evaluated in this article, or claim that may be made by its manufacturer, is not guaranteed or endorsed by the publisher.

Copyright © 2022 Ni, Dong, Yao, Chen, Liang, Liu, Li, Guo and Gao. This is an open-access article distributed under the terms of the Creative Commons Attribution License (CC BY). The use, distribution or reproduction in other forums is permitted, provided the original author(s) and the copyright owner(s) are credited and that the original publication in this journal is cited, in accordance with accepted academic practice. No use, distribution or reproduction is permitted which does not comply with these terms.